Coupling a proton and a neutron to the semidoubly magic nucleus ^{68}Ni: A study of ^{70}Cu via the β decay of ^{70}Ni and ^{70}Cu

J. Van Roosbroeck,* H. De Witte, M. Gorska, M. Huyse, K. Kruglov, K. Van de Vel, and P. Van Duppen
Instituut voor Kern- en Stralingsfysica, University of Leuven, Celestijnenlaan 200D, B-3001 Leuven, Belgium

S. Franchoo, J. Cederkall, V. N. Fedoseyev, H. Fynbo, U. Georg, O. Jonsson, and U. Köster
ISOLDE, CERN, 1211 Genève 23, Switzerland

L. Weissman and W. F. Mueller
National Superconducting Cyclotron Laboratory, Michigan State University, 164 S. Shaw Lane, Michigan 48824-1312, USA

V. I. Mishin
Institute of Spectroscopy, Russian Academy of Sciences, 142092 Troitsk, Russia

D. Fedorov
St. Petersburg Nuclear Physics Institute, 188350 Gatchina, Russia

W. B. Walters
Department of Chemistry, University of Maryland, College Park, Maryland 20742, USA

N. A. Smirnova, A. Van Dyck, A. De Maesschalck, and K. Heyde
Vakgroep Subatomaire en Stralingsfysica, Universiteit Gent, Proeftuinstraat 86, B-9000 Gent, Belgium
(IS365 Collaboration and ISOLDE Collaboration)
(Received 20 November 2003; published 10 March 2004)

The ^{70}Ni nucleus has been produced at the LISOL facility and its β decay to ^{70}Cu has been observed. In parallel, the ^{70}Cu nucleus has been produced at the ISOLDE facility. A new third β-decaying isomeric state in ^{70}Cu has been identified, partly with the aid of the in-source laser spectroscopy method. Its measured half-life is $T_{1/2}=33(2)$ s. In addition, two isomeric transitions in ^{70}Cu have been observed at energies of 101.1(3) and 141.3(3) keV, and it allowed the relative placement of the three ^{70}Cu isomeric states and their tentative spin and parity assignments. The new ^{70}Cu isomer was found to be weakly populated in the β decay of ^{70}Ni. It allowed the construction of the ^{70}Ni decay scheme. Furthermore, the β decay of the three ^{70}Cu isomers to ^{70}Zn has been measured and their decay schemes are presented. The ^{70}Ni β decay to the isomeric states in ^{70}Cu and their subsequent isomeric decay and β decay to ^{70}Zn are discussed within the extreme shell-model picture of two valence nucleons outside the semidouble magic $^{68}_{28}$Ni$_{40}$ core and it yields satisfactory results. Large-basis shell-model calculations using $^{56}_{28}$Ni$_{28}$ as the core and a realistic effective interaction support rather well the suggested interpretation.

DOI: 10.1103/PhysRevC.69.034313 PACS number(s): 21.10.−k, 23.40.−s, 25.85.Ec, 27.50.+e

I. INTRODUCTION

Recent in-beam [1–7] and decay studies [8–13] revealed various features of the nuclear structure in the vicinity of the semidouble magic nucleus $^{68}_{28}$Ni$_{40}$. This nucleus exhibits some characteristics of a doubly magic nucleus [e.g., the excitation energy of the 2^+_1 state, $E(2^+_1)$, is raised by more than 500 keV in ^{68}Ni in comparison with ^{66,70}Ni [1,3]]. Yet, the stabilizing effects are weak (see, e.g., the two-neutron separation energies and their differences [14]) and disappear with the addition of a single nucleon [10]. The apparent doubly magic properties of the ^{68}Ni nucleus are attributed to the single-particle energy gap at $N=40$ and to the occurrence of a change in parity between the pf orbitals ($\pi=-$) and the intruder g orbital ($\pi=+$) across the $N=40$ gap. The latter effect is illustrated by the reduced $E2$-transition probability, $B(E2:0^+_1\rightarrow 2^+_1)$, observed in ^{68}Ni. Its $B(E2)$ value is as low as in the cases of "real" doubly magic nuclei [7] and it is understood in view of the above parity change [17]. A recent study suggested that the $B(E2)$ value to the first excited 2^+ state forms only part of the low-lying $B(E2)$ strength and it therefore is argued that the small experimental $B(E2)$ value cannot be used as a strong evidence for the double-magic character of ^{68}Ni [15]. The poorly known residual interaction between the (quasi)particle and hole states in this region of the nuclear chart, which influences also stellar collapse models [16], gives rise to the above mentioned apparent controversial situation. The weakness of the stabilizing effects at $N=40$ can be attributed to the small single-particle energy gap ($\sim$2 MeV) in comparison with energy gaps near full

*Corresponding author. Email address: piet.vanduppen@fys.kuleuven.ac.be

shell closures (>3 MeV). Hence, the terms subshell and semidouble magic nucleus are used.

In this work, we address the question whether the $^{70}_{29}Cu_{41}$ nucleus can be interpreted in terms of an inert $^{68}_{28}Ni_{40}$ core plus two valence nucleons. If ^{68}Ni is a well-suited core nucleus, the states in ^{70}Cu can be interpreted as originating from the coupling of the valence proton with the valence neutron into spin multiplets. These multiplets split up in energy, due to the residual proton-neutron interaction, with a parabolic $I(I+1)$ dependence in the simplest approach [18]. Similarly, the β decay of ^{70}Ni to states in ^{70}Cu and the subsequent β decay of ^{70}Cu to ^{70}Zn should equally fit within this picture and the β^- decay should selectively probe specific structures.

The β decay of ^{70}Ni has already been measured at LISOL by Franchoo *et al.* [8,12] but only the production rate and the half-life [$T_{1/2}$=6.0(3) s] have been reported. In addition, several excited states in the ^{70}Cu daughter nucleus populated via the $(t,{}^3\mathrm{He})$ reaction on ^{70}Zn have been reported by Sherman *et al.* [19]. Furthermore, the ^{70}Cu nucleus is known to have two β-decaying isomers [20–22]. The spin and parity (I^π) of the isomers were assigned (1^+) and $(4)^-$ [23]: the (1^+) isomer being the ground state or *g* isomer with a $T_{1/2}$=45(10) s half-life; the $(4)^-$ state or *m* isomer at 140(80) keV above the *g* isomer [21] with a $T_{1/2}$=47(5) s half-life. The proposed difference in parity implies different shell-model configurations for both isomers: it was suggested that the *g* isomer consists mainly of a $\pi 2p_{3/2}\nu 2p_{1/2}^{-1}1g_{9/2}^{+2}$ configuration whereas the *m* isomer has mainly the $\pi 2p_{3/2}\nu 2p_{1/2}^{+2}1g_{9/2}^{+1}$ shell-model configuration. The β decay of both ^{70}Cu isomers to ^{70}Zn has been reported in Refs. [20–22]. Since ^{70}Zn is a stable nucleus, it has been investigated intensively using reaction studies as well, e.g., Refs. [6,24–26]. Consequently, many excited states in ^{70}Zn have been established; the I^π and $B(E2)$ values of several levels have been deduced.

The ^{70}Ni β decay and the subsequent β decay of the ^{70}Cu isomers are studied in more detail in order to gain further insight into the structure of these nuclei. The ^{70}Ni and ^{70}Cu nuclei were both produced using a proton-induced fission reaction of uranium but at different facilities, applying different methods. The production of ^{70}Cu was done at a thick-target facility such as ISOLDE at CERN (Geneva, Switzerland) [27]. A thick target allows high production rates, and in combination with a sufficiently fast release time of copper from the target (ca. 13 s), high copper yields can be achieved. Furthermore, resonant laser ionization is applied in order to obtain relatively clean copper beams [28,29]. Yields of 9×10^7 μC^{-1} of ^{70}Cu are obtained [30]. A disadvantage is that elements with a low ionization potential (Ga, Rb,…) are easily surface ionized in the hot ionizer cavity of the ISOLDE ion source. This often causes significant beam contaminations. The release time from the target for neighboring nickel is much longer and therefore the production of short-lived nickel isotopes is preferentially done with an alternative method such as the thin-target gas cell method used, e.g., at the LISOL facility [31]. The target here is made sufficiently thin in order for the reaction products to escape. The fission fragments are subsequently thermalized and neutralized in a buffer gas (500 mbar Ar). The main advantage of this method is that the extraction time from the gas cell is fast (200–500 ms) and does not depend on the chemical properties of the reaction products. This makes the method rather universal. A drawback is that the yield is limited by the effective target thickness ($\approx$10 mg/cm^2), determined by the range of the reaction products in the target. In combination with resonant laser ionization [31], the final beam can be made sufficiently clean. With this method, ion yields of 28(5) and 12(2) μC^{-1} can be achieved for ^{70}Ni and ^{70}Cu, respectively [32,33]. In spite of the low yields compared with ISOLDE, the gas cell approach offers the best alternative for producing isotopes which have slow release times in the thick-target method. For this reason, the ^{70}Ni nucleus was studied at the LISOL facility.

The β decay of both ^{70}Ni and ^{70}Cu isotopes was examined using β-γ and γ-γ-spectroscopy. In addition, the relatively new technique of in-source laser spectroscopy [13,34,35] was exploited on the ^{70}Cu isotope at ISOLDE. This method enables one to probe the hyperfine splitting (HFS) of atomic states using a narrow-band laser in the first excitation step in the resonant laser ionization process and was used to extract magnetic moments of isomeric and ground states in ^{68,70}Cu [13,34,35]. The method further allows one to separate radiation originating from different isomers in a particular isotope. The combination of both β-decay and in-source laser spectroscopy has led to the discovery of a third isomeric state in ^{70}Cu.

In Sec. II, we present the ^{70}Ni β-decay data from the experiments at LISOL and the ^{70}Cu β-decay data from the ISOLDE experiments. We further present evidence for the existence of a third β-decaying isomer in ^{70}Cu. We argue the relative placement and spin assignments of the three ^{70}Cu isomers. In addition, the detailed decay schemes of the ^{70}Ni and the three ^{70}Cu isomeric decays and the extracted half-lives and production rates of the three ^{70}Cu isomers are presented. In Sec. III, the results are interpreted within an extreme shell-model picture and a large-basis shell-model calculation.

II. RESULTS

A. Experimental setup

The experimental setup used in the β-decay study of ^{70}Ni at LISOL is described in detail in Ref. [12] and is not repeated here. Fission was induced by impinging a 30 MeV proton beam with a typical dc intensity of 10 μA on two foils of natural uranium with a thickness of 10 mg/cm^2. The experimental setup used for the decay study of ^{70}Cu is discussed in detail below.

In a first experiment, a pulsed beam of 1 GeV protons was impinging on a standard ISOLDE uranium carbide target (50 g/cm^2 U) [36]. In a second experiment, a proton-to-neutron converter was used to induce fission with low-energy neutrons in order to suppress some disturbing high-energy proton-induced fission products such as ^{70}Ga in this case [37]. The converter consists of a Ta rod, mounted at 24 mm (axis to axis) in parallel to the target. Only the low-energy spallation neutrons, with some MeV energy, are able to reach

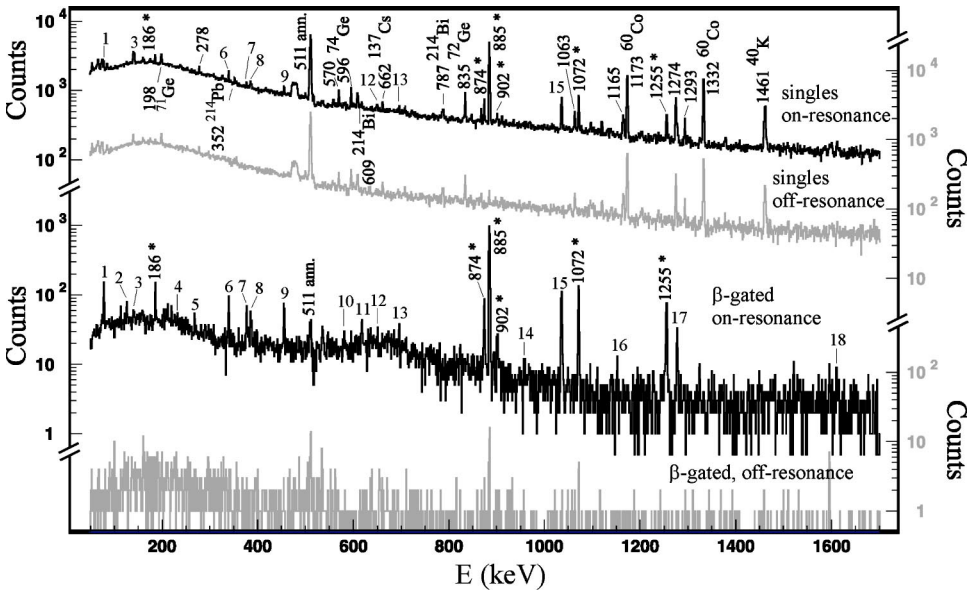

FIG. 1. On- and off-resonance singles and β-gated γ-ray spectra, taken on mass $A=70$ with the lasers set to ionize nickel. Lines labeled with a number are attributed to the β decay of ^{70}Ni and are listed in Table I; lines labeled with "*" originate from the decay of the ^{70}Cu daughter nucleus.

the target while the primary beam and the high-energy neutrons are strongly forward peaked, mainly in a cone which does not hit the target. In both cases, the fragments from the fission reaction diffused out of the target which was heated to about 2000 °C. They were guided to the RILIS ion source (resonance ionization laser ion source) [28,29] where the copper atoms were resonantly laser ionized by means of two laser beams of 327.4 nm and 287.9 nm wavelength. After extraction with a 60 kV voltage and mass separation, the ^{70}Cu isotopes were guided to different experimental setups.

A first setup was used to perform in-source laser spectroscopy measurements [13,34,35]. For this method, the first step laser was operated in narrow bandwidth mode (bandwidth 1.2 GHz). The frequency was scanned in a range of 20 GHz in order to probe the HFS of the ground and first excited atomic states. For the second step laser, a broadband (24 GHz) dye laser was used. The ^{70}Cu yield as a function of the first step laser frequency was monitored in a β-γ-detection setup. It consists of a movable tape that transports the implanted activity into a 4π cylindrical β detector, positioned next to a 30% relative efficiency Ge(Li) detector. For each laser frequency setting, several measurements were performed to average over possible yield fluctuations. Furthermore, the ion current of stable ^{63}Cu was measured simultaneously at a different beam line in order to detect fluctuations in the copper yield.

A second setup was used for decay-spectroscopy measurements. In this case, the first step laser was switched to a broad bandwidth in order to maximize the ionization of copper. The extracted ^{70}Cu isotopes were then implanted on a tape, surrounded at close distance by three thin plastic ΔE detectors for β detection (solid angle $\sim$50% of 4π) and two HPGe detectors (64% and 75% or 75% and 90% relative efficiency for the different experiments, respectively).

B. The β decay of ^{70}Ni studied at LISOL

Data on mass $A=70$ were collected at LISOL in a cyclic mode using a 24 s implantation and 40 s decay period. The proton beam had an additional microstructure during the implantation period in which it was switched on for 250 ms and subsequently switched off for 250 ms [12]. Representative singles and β-gated γ-ray spectra are shown in Fig. 1. The singles spectra are the total sum of different spectra, taken during different time intervals of each 8 s long. These so-called multiscaling spectra divide the implantation and decay period in eight different slices in order to monitor the time dependence of the γ-ray intensities. The figure shows both the on-resonance (the lasers are switched on) and the off-resonance spectra (the lasers are switched off). The laser frequencies were tuned to ionize nickel. The measuring time for the on-resonance spectra is 324 min and 120 min for the off-resonance spectra. The average proton beam current during the time the beam was switched on was 10.1 μA during the on-resonance measurement and 10.3 μA during the off-resonance measurement.

If one compares the β-gated on- and off-resonance spectra from Fig. 1, one observes a number of lines that appear only in the on-resonance spectra. These lines necessarily come from the ^{70}Ni β decay and related daughter activity. The lines attributed to the ^{70}Ni β decay are labeled with a number and their properties are listed in Table I. The transitions labeled with "*" were found to originate from the β decay of the ^{70}Cu daughter nucleus, based on their coincidence relations with the $2^+ \rightarrow 0^+$ transition in ^{70}Cu at 885 keV. The ^{70}Cu activity is present both when the lasers are on- and off-resonance [12]. This indicates that part of the ^{70}Cu nuclei survive the thermalization process as 1^+ ions in the gas cell and are mass separated.

The singles γ-ray spectra in Fig. 1 contain various extra lines compared to the β-gated spectra. Several transitions were found to originate from room background, e.g., the 1461 keV line from ^{40}K, or originate from neutron reactions, e.g., the 596 keV line from the ^{73}Ge$(n,\gamma)^{74}$Ge reaction. The neutrons stem from nuclear reactions at the proton beam dump or from the fission reaction of uranium. Most background- and neutron-induced γ lines are present both in the on- and off-resonance spectra, as expected.

TABLE I. Energy values, peak areas from the on-resonance β-gated γ-ray spectrum, half-lives values, and coincident γ rays of the lines observed in the decay of ^{70}Ni (see text). The peak areas of coincident γ rays are shown in brackets.

Label	E (keV)	Area	$T_{1/2}$ (s)	Coincident γ rays
1	78.3(1)	198(24)	6(2)	340(59), 377(84), 386(12), 618(36), 957(9)
2	126.5(2)	66(23)	9(4)	140(36), 1152(9), 1611(10)
3	140.4(6)	44(27)	18.7(7)	127(33), 1152(3), 1611(5)
4	232.8(3)	24(5)		78(5), 340(11), 386(11)
5	267.8(4)	24(5)	30(21)	1152(6), 1611(9)
6	339.6(1)	138(23)	5.6(13)	78(54), 233(11), 386(16), 618(65), 696(60)
7	377.2(1)	98(25)	5(3)	78(80), 581(11)
8	385.7(5)	72(17)	16(12)	78(13), 233(18), 340(10), 650(41)
9	455.1(1)	134(20)	4(2)	581(15)
10	581.1(2)	23(5)		78(4), 377(11), 455(14)
11	618.4(2)	66(20)	4.1(14)	78(31), 340(66)
12	650.1(2)	21(5)		386(37)
13	696.1(1)	36(6)		340(55)
14	956.9(3)	9(5)		78(8)
15	1035.6(2)	241(15)	6.2(3)	
16	1152.3(4)	21(7)	6(5)	127(7), 140(4), 268(6)
17	1277.6(2)	66(9)	13(2)	
18	1611.2(3)	14(4)		127(8), 140(4), 268(8)

Table I lists the peak properties of the lines attributed to the decay of ^{70}Ni. It contains the peak labels, the energies, the areas, half-lives, and the coincident γ rays. The peak areas are extracted from the on-resonance β-gated γ-ray spectrum in Fig. 1, using a proper background subtraction. The half-life values were extracted using a single-component exponential decay fit of the time dependence of the γ-ray peak areas, obtained from the multiscaling spectra. If no half-life value was specified, the peak area would be too weak to determine the half-life value. The coincident γ-rays were obtained from γ-ray gated γ spectra, using a proper background subtraction in order to eliminate coincident events related to background beneath the peak.

All half-life values, shown in Table I, agree within the error with the $T_{1/2}=6.0(3)$ s half-life from ^{70}Ni except line number 3 at 140.4 keV. Its apparent half-life is significantly longer. Notice that this line is only weakly present in the β-gated spectrum but it is quite intense in the singles spectrum. The half-life values were extracted using the singles spectra and therefore the diverging half-life hints the existence of a doublet line. The excess of peak counts in the singles spectrum was found to originate partly from an isomeric transition in ^{70}Cu at 141.3(3) keV and partly from a neutron capture induced γ line at 139.7 keV. As will be shown further, the 141.3(3) keV γ ray is a transition between two isomers in ^{70}Cu and the decaying isomer has a half-life of $T_{1/2}=6.6(2)$ s. It is produced in the ^{70}Ni β decay and therefore only appears in the on-resonance spectrum. There is however also a nonresonant contribution in the singles spectra and this is attributed to an isomeric transition in ^{75}Ge having a 47.7 s half-life [23]. This nucleus is presumably produced via the ^{74}Ge$(n,\gamma)^{75}$Ge neutron reaction in the Ge crystal of the γ detectors. The observed longer half-life of the line near 140 keV, shown in Table I, can thus be attributed to the combined effects described above.

C. The β decay of ^{70}Cu studied at ISOLDE

The β decay of ^{70}Cu was performed at ISOLDE. A representative singles spectrum (measuring time $\Delta t=33$ min) is compared with a β-gated spectrum ($\Delta t=4$ min) in Fig. 2. Both spectra were collected on mass $A=70$ with the lasers tuned to ionize copper. No off-resonance spectra have been collected. In this particular case, the first step laser was operating in the way it was used during the in-source laser spectroscopy measurements, i.e., with reduced power and in narrow bandwidth mode. The laser frequency setting for this measurement was $1/\lambda=30\,534.96$ cm^{-1}. Furthermore, neutron-induced fission was applied, by introducing the proton-to-neutron converter next to the target, as described above. The used time cycle consisted of a 3.45 s implantation and a 0.4 s decay period. The beam gate of the separator was opened only 50 ms after the time of impact of the primary proton beam pulse.

Transitions that are attributed to the β decay of ^{70}Cu are labeled with a number in Fig. 2. These γ rays are present both in the singles and the β-gated spectra. Their properties are listed in Table II. The lines at 1787, 2137, and 2154 keV are found to be pure sum peaks of the three most intense γ rays from the β decay of ^{70}Cu, i.e., the 885, 902, and 1252 keV transitions. The sum peaks are labeled with "Σ-line" in the figure. The lines not attributed to the β decay of ^{70}Cu are labeled with their energy and decay parent, when known. Most of these lines are room background or come from long-lived activity that was implanted next to the tape during the measurement or preceding measurements. In most

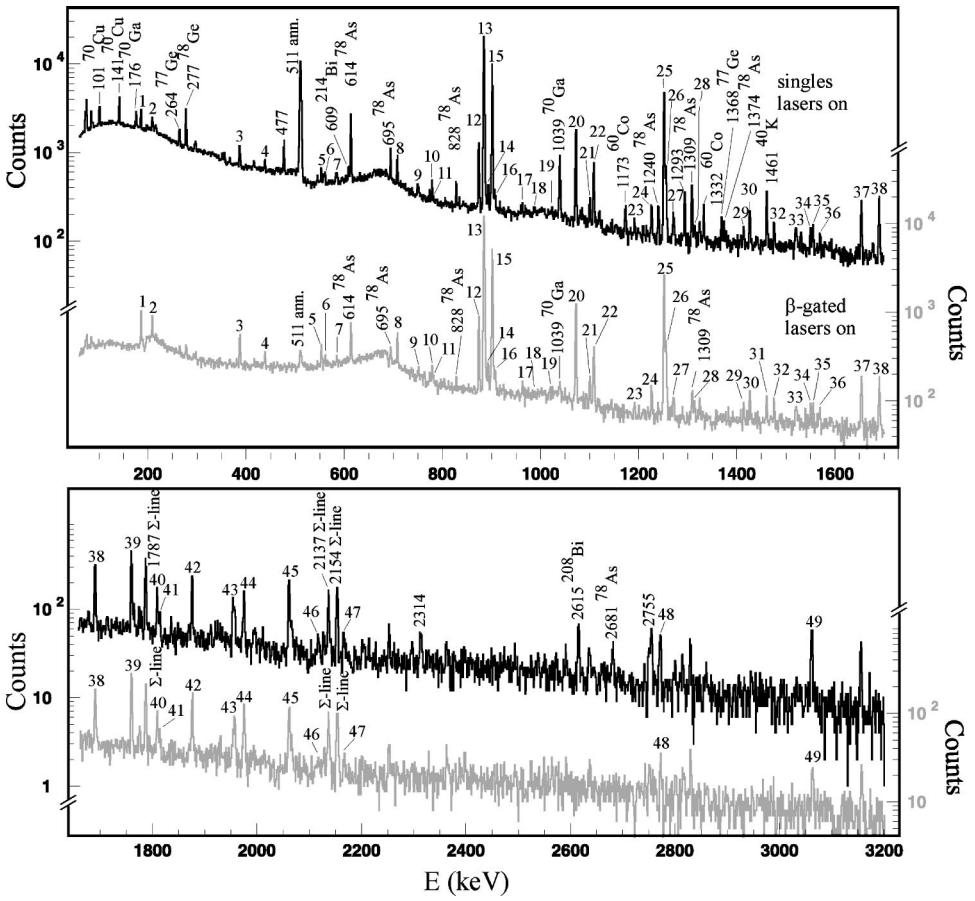

FIG. 2. Singles and β-gated γ-ray spectra taken on mass $A=70$ with the lasers set to ionize copper. The first step laser was operated with reduced power and in narrow bandwidth at a frequency setting of $1/\lambda = 30\,534.96\ \mathrm{cm}^{-1}$. Lines labeled with a number are attributed to the β decay of ^{70}Cu and are listed in Table II. Lines labeled with "Σ-line" are sum lines from intense transitions originating from the decay of ^{70}Cu.

cases, these are members of the decay chains of the gallium isotopes since surface ionized gallium is the major beam contaminant for masses $A \geqslant 74$. Several long-lived contaminations on masses $A=77$ and 78 (e.g., ^{78}As) are found in the spectra since prior to this measurement an intensive study of the ^{77,78}Cu isotopes was made. In some cases, e.g., in the ^{70}Ga β decay, γ-ray transitions are strongly reduced in the β-gated spectrum in comparison to the singles spectrum. This is because the radioactive source was implanted next to the tape and too far away for a β particle to reach the ΔE detectors, as the ΔE detector setup was optimized for sources implanted onto the tape.

The γ rays at energies of 101.1(3) and 141.3(3) keV, present in the singles spectrum in Fig. 2, are absent in the β-gated spectrum. The intensities of these γ lines show a definite laser frequency dependence, as shown below, and are therefore related to the ^{70}Cu decay. Hence, these are delayed isomeric transitions in ^{70}Cu or in the stable ^{70}Zn daughter nucleus fed through the β decay of ^{70}Cu. Moreover, the 141.3(3) keV transition was also observed in the ^{70}Ni decay. The origin of these γ lines is discussed in the following section.

The peak areas shown in Table II are extracted from the singles spectrum in Fig. 2. The half-life values are derived from a single-component exponential decay fit of the time dependence of the γ-ray intensities, derived from a data set having a 250 s long decay period. The coincident γ rays are found by making γ-gated γ-ray spectra with a prompt gate ($\sim$100 ns time window) on the time-to-amplitude-converter spectrum. A proper correction for the background under the peaks was performed. For some γ rays, there is only a weak sign for a coincidence; their peak area is indicated with "-."

Considering the coincident γ rays from the transitions shown in Table II, one observes that all 49 γ rays exhibit mutual coincidence relations with known intense ^{70}Cu γ rays (885, 902 keV, etc.) [38]. It confirms that all these lines originate from the ^{70}Cu β decay. The half-life of most γ rays agrees within the errors with the 47(5) s half-life of the m-isomeric state in ^{70}Cu reported in Ref. [20]. Only two γ rays, the 186 keV and the 1876 keV transitions, exhibit a short half-life, agreeing with the 4.5(10) s half-life of the g isomer. Several γ rays, however, have a half-life value that lies in between the two known half-lives, disagreeing with both half-lives from literature. Either their time dependence is a mixture of the two half-life values or it indicates the existence of another decaying isomer in ^{70}Cu or in the ^{70}Zn daughter nucleus. In the following section, we will show that there indeed exists a third isomer in ^{70}Cu with a half-life different from 4.5 and 47 s.

D. Search for a new isomer in ^{70}Cu

Support for the existence of a new third isomer in ^{70}Cu is found by analyzing the dependence of the ^{70}Cu γ rays on the frequency of the first step laser. This is the so-called in-source laser spectroscopy method [13]. For each frequency setting, three independent measurements of 10 s each are combined. For each measurement, there was a single implan-

TABLE II. Energy values, peak areas from the on-resonance singles spectrum, half-lives values, and coincident γ rays of the lines observed in the decay of ^{70}Cu (see text). The peak areas of coincident γ rays are shown in brackets.

Label	E (keV)	Area	$T_{1/2}$ (s)	Coincident γ rays
1	185.85(3)	2101(106)	6(3)	885(137)
2	208.75(7)	1469(102)	30(3)	885(160), 902(200), 1252(162)
3	387.10(5)	958(70)	24(2)	885(127), 902(47), 1072(43), 1101(21), 1760(10), 1975(30)
4	438.2(2)	399(62)	66(12)	885(178), 902(145), 1252(107), 1315(12)
5	553.2(1)	394(51)	17(5)	885(85), 902(19), 907(39), 1809(30)
6	560.82(8)	221(48)	43(6)	885(71), 902(81), 1252(102)
7	584.7(1)	441(61)	36(6)	438(12), 885(75), 902(63), 1252(30), 1690(35)
8	708.42(7)	1164(72)	27(2)	779(46), 885(130), 1654(88)
9	750.0(2)	310(46)	39(5)	885(85), 902(101), 1252(−)
10	779.1(2)	362(41)	43(10)	708(45), 874(13), 885(−), 1760(10)
11	783.1(2)	56(39)	169(132)	885(−), 902(−), 1809(14)
12	874.33(8)	2428(68)	16(2)	708(24), 779(25), 885(205), 1101(27), 1876(12)
13	884.88(9)	45387(221)	47.6(8)	186(50), 209(100), 387(130), 438(178), 553(82), 561(93), 708(141), 750(123), 874(205), 893(135), 902(7762), 907(257), 963(69), 1023(54), 1072(381), 1108(580), 1192(49), 1226(106), 1252(3828), 1255(149), 1271(103), 1315(48), 1414(46), 1427(133), 1476(72), 1520(66), 1551(44), 1570(30), 1654(82), 1690(301), 1809(100), 1815(55), 1954(78), 1975(61), 2062(215), 2154(1206), 2771(40), 3062(64)
14	893.1(6)	357(40)	54(5)	885(163), 902(128), 1108(143),1271(15)
15	901.7(1)	21161(153)	51.5(8)	209(80), 438(150), 561(70), 585(75), 750(85), 885(7940), 893(73), 907(113), 963(63), 1072(103), 1108(584), 1192(65), 1226(101), 1252(3917), 1271(116), 1427(109), 1476(82), 1520(74), 1551(56), 1690(266), 1815(47), 1954(116), 2062(167), 2117(31), 2137(127), 2771(49), 3062(68)
16	906.5(1)	277(37)	45(8)	553(15), 783(6), 885(79), 902(60)
17	963.3(1)	149(34)	28(9)	885(59), 902(59), 1252(46)
18	988.0(3)	144(38)	35(11)	438(10), 885(37), 902(20), 1690(13)
19	1023.3(2)	62(33)	50(34)	885(45), 902(48), 1252(14)
20	1072.2(1)	4222(77)	18(2)	387(55), 885(352), 902(55)
21	1100.5(2)	297(37)	35(12)	387(23), 874(23), 885(53)
22	1108.4(1)	1430(53)	53(3)	885(595), 893(120), 902(540), 1414(15), 1570(40), 1815(47), 1954(15), 2166(22)
23	1191.5(2)	145(31)	33(6)	885(55), 902(37)
24	1226.3(7)	382(32)	63(14)	885(128), 902(108), 1252(75)
25	1251.7(1)	11049(106)	54(1)	209(87), 438(114), 561(71), 585(27), 750(52), 885(3836), 902(3767), 963(49), 1023(27), 1226(93), 1271(58), 1427(102), 1476(49), 1520(38), 1551(36), 1787(130)
26	1255.4(2)	1501(161)	20(4)	885(35)
27	1270.8(2)	290(28)	61(11)	885(74), 902(87), 1252(50)
28	1315(1)	133(24)	100(70)	885(19), 902(17), 907(4), 1690(18)
29	1413.9(2)	123(27)	54(30)	885(26), 902(20), 1108(21), 1787(6)
30	1426.5(2)	375(32)	45(5)	885(90), 902(77), 1252(98)
31	1460.4(2)	741(39)	26(9)	885(16), 902(26)
32	1476.1(2)	217(29)	62(18)	885(80), 902(78), 1252(45)
33	1520.1(3)	244(33)	65(31)	885(37), 902(53), 1252(34)
34	1550.6(3)	203(30)	84(46)	885(50), 902(70), 1252(29)

TABLE II. (*Continued.*)

Label	E (keV)	Area	$T_{1/2}$ (s)	Coincident γ rays
35	1555.2(3)	197(25)	72(29)	885(31), 902(49)
36	1569.8(2)	100(27)	79(25)	885(37), 902(48), 1108(36)
37	1653.9(2)	516(35)	30(4)	708(90), 885(77)
38	1690.3(2)	733(37)	54(5)	585(25), 885(264), 902(235), 1787(10)
39	1759.6(2)	1007(40)	16(4)	708(12), 1101(6), 1876(8)
40	1809.1(5)	108(23)	28(5)	553(26), 783(9), 885(75)
41	1815.0(5)	532(31)	52(14)	885(54), 902(50), 1108(33)
42	1875.8(2)	426(32)	3(6)	874(16), 885(15), 1760(13)
43	1954.2(3)	412(32)	52(8)	885(104), 902(85), 1108(17)
44	1975.0(4)	569(31)	26(4)	387(26), 885(50)
45	2061.6(6)	58(15)	52(5)	885(138), 902(124), 1787(6)
46	2117.2(4)	96(16)	116(129)	885(16), 902(9)
47	2166.2(5)	110(14)	26(14)	885(17), 902(17), 1108(12)
48	2771.2(6)	249(17)	35(12)	885(44), 902(45)
49	3062.1(6)	285(17)	51(11)	885(68), 902(46)

tation period of 1 s and a 9 s decay period. Three groups of γ rays were found, see Fig. 3, exhibiting different HFS. Previously, only the HFS of parts (a) and (c) of Fig. 3 had been observed [34,35] and they were related to the g and m isomers in ^{70}Cu, respectively. It can be seen from the half-lives of the γ rays that the 186 keV and the 1876 keV γ rays in part (a) of the figure show a half-life agreeing with the 4.5(10) s of the g isomer (see Table II); the 1252 keV, 1690 keV, and the 1108 keV γ rays in part (c) exhibit a half-life matching with the 47(5) s of the m isomer. Several other γ-rays showing the same HFS were found but are not shown in part (c) of the figure. Part (b) shows a new and larger HFS, and is therefore evidence for the existence of a third isomer in ^{70}Cu. An isomeric state in the zinc daughter is excluded because the laser scheme is tuned only to ionize copper. The extracted HFS and magnetic moments of the three ^{70}Cu isomers are presented in Ref. [13]. The isomeric transitions at 101 and 141 keV, discussed in the preceding section, depend on the laser frequency and show different HFS. Therefore, both transitions are related to the decay of different isomers. The laser frequency dependence of the 141 keV isomeric transition is shown in part (a) of the figure and the transition can therefore be assigned to the decay of the g isomer in ^{70}Cu. Hence, it can no longer be called the ground-state isomer. The 101 keV isomeric transition shows the new HFS [part (b)] and is therefore originating from the new isomer. The half-life deduced for the other γ rays in part (b) are all consistent with the previously observed new half-life of roughly 25–30 s. Apart from the γ rays shown in part (b), several other γ rays were found, exhibiting clearly the same HFS and half-life: 209, 387, 553, 708, 779, 1101, 1192, 1460, 1654, and 1975 keV. Since these transitions were already assigned to the β decay of ^{70}Cu, we can state that the new isomer decays both by γ and β decays.

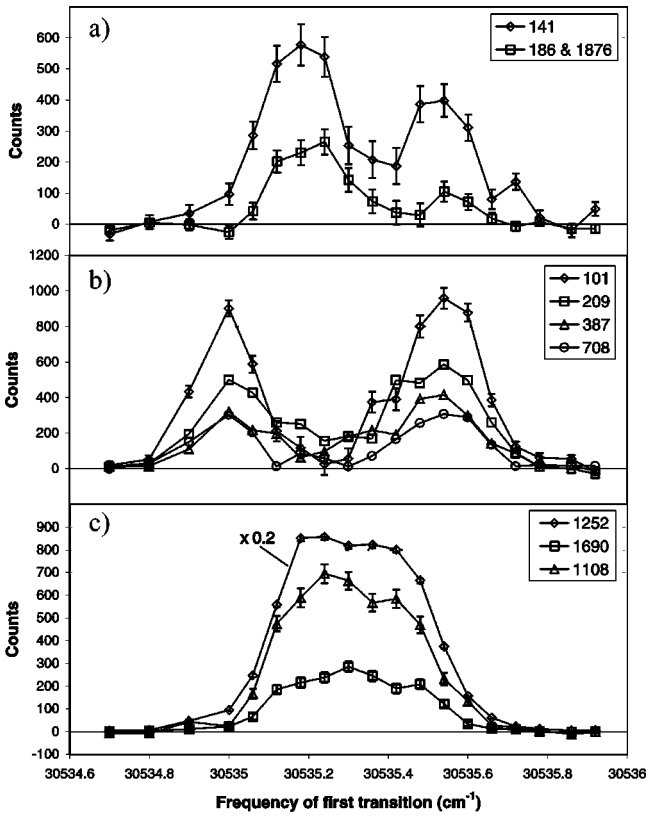

FIG. 3. Laser frequency dependence of several γ rays from ^{70}Cu. The γ rays are grouped in three categories, according to their hyperfine splitting (HFS). Values for the 1252 keV γ ray are scaled down by a factor of 5. (b) represents the HFS of the new isomer in ^{70}Cu.

It is instructive at this point to refer to some earlier observations. In the work of Ref. [20], spectroscopic measurements were done on a sample enriched with ^{70}Zn, activated by 14 MeV neutrons. Several γ rays were assigned to the two known ^{70}Cu isomers, mainly based on the half-life. However, 16 other γ rays, among which a 100.0(4) keV, a 140.6(8) keV, and several other lines from the above list or

from Table II were assigned to ^{67}Ni because their diverging half-lives agreed better with its 18(4) s half-life. The ^{67}Ni nucleus was assumed to be produced via the ^{70}Zn(n,α) reaction. The same experiment was repeated [21] and also here, a third β and γ activity of $T_{1/2}$16(4) s was observed and attributed to ^{67}Ni. However, in Ref. [22], this activity was reassigned to ^{70}Cu because the γ rays of 208.4, 708.2, 1072.2, and 1654.1 keV in mass-separated samples at mass 70 was observed. The diverging half-life was explained to be a mixture of the two known ^{70}Cu isomers. In view of the present discussion, it is clear that the wrongly assigned ^{67}Ni activity was the activity from the newly identified, third isomer in ^{70}Cu.

E. Relative placement of the three ^{70}Cu isomers

For reasons of simplicity, we will reassign new labels to the three isomers in ^{70}Cu and call them ^{70a,b,c}Cu, corresponding to the labels of the three different parts in Fig. 3. Since ^{70c}Cu is the only isomer which does not decay via an isomeric transition, it could be the ^{70}Cu ground state. This is not in agreement with the conclusion from the β-end-point measurements [21] but the large uncertainty on the energy [140(80) keV] allows this interpretation. The ^{70a,b}Cu isomers are linked, respectively, to the 141 and 101 keV isomeric transitions. No other γ rays were found to be coincident with the two isomeric transitions, so the transitions are feeding directly onto another isomer.

The relative placement of the three isomers is suggested by the ^{3}He spectrum from the $(t,{}^3\mathrm{He})$ reaction on ^{70}Zn from Sherman *et al.* [19]. This spectrum shows five resonances at relative energies of 0.0, 100(6), 226(6), 366(6), and 506(6) keV, respectively. The multiplets of states at energies of 0.0, 100(6), 226(6), and possibly 506(6) keV are strongly populated and are therefore claimed to have a $\pi 2p_{3/2}\nu 1g_{9/2}$ shell-model configuration, based on similar observations in the ^{64,66,68}Cu nuclei [19]. It was not sure whether the state labeled with 0.0 is the actual ground state. However, since the ^{70c}Cu isomer—the former *m* isomer—is thought to have the $\pi 2p_{3/2}\nu 1g_{9/2}$ configuration [20] and since the ISOLDE data suggest it to be the ground-state isomer, we claim that it actually is the lowest-energy state. The energy difference between the two lowest states in the $(t,{}^3\mathrm{He})$ spectrum is 100(6) keV, agreeing with the energy of the 101 keV isomeric transition from our data, connected to the decay of the ^{70b}Cu isomer. It implies that this ^{70b}Cu isomer corresponds to the state at 100(6) keV from the ^{3}He spectrum and that also this isomer belongs to the same $\pi 2p_{3/2}\nu 1g_{9/2}$ multiplet, forcing it to have negative parity as well.

In the assumption that both ^{70b,c}Cu isomers have a pure $\pi 2p_{3/2}\nu 1g_{9/2}$ shell-model configuration, it is possible to calculate their magnetic moments in the single-particle model using the additivity relation. The predictions can then be compared with the measured ^{70b,c}Cu magnetic moments from the in-source laser spectroscopy method, as shown in Ref. [13], and it allows us to attribute a spin parity of (3^-) and (6^-) to the ^{70b,c}Cu isomers, respectively.

Finally, we note that Ishii *et al.* came to the same conclusions regarding the spin assignments when they discuss the

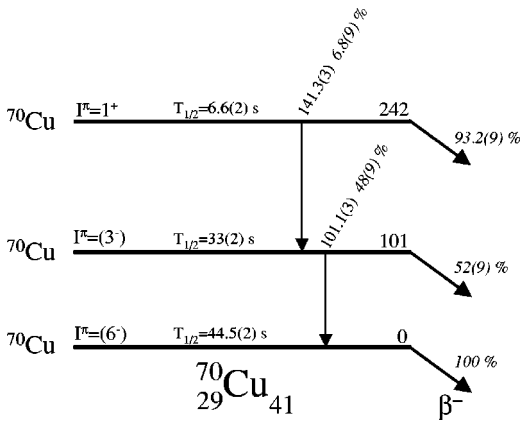

FIG. 4. The deduced relative placement for the ^{70}Cu isomers and their decay properties. The branching ratios for the isomeric transitions contain an internal conversion correction [42].

members of the $\pi 2p_{3/2}\nu 1g_{9/2}$ multiplet from the $(t,{}^3\mathrm{He})$ reaction data [39].

The third ^{70a}Cu isomer is presumed to be a (1^+) state from the $\pi 2p_{3/2}\nu 2p_{1/2}^{-1}$ doublet. This is again supported by comparing the deduced magnetic moment with the calculated magnetic moment using the additivity relation [13]. The isomer is expected to be only weakly produced in the $(t,{}^3\mathrm{He})$ reaction and therefore it is most likely not observed in the ^{3}He spectrum in Ref. [19]. The 141 keV isomeric transition however suggests the ^{70a}Cu isomer to be located 141 keV above the ^{70b}Cu isomer, resulting in a delayed *M*2 transition between the (1^+) and (3^+) states. Notice that the decay of the (1^+) isomeric state to the (6^-) ground state will not be observed because of the large multipolarity of the transition (*E*5). It rules out the placement of the ^{70a}Cu isomer 141 keV above the ^{70c}Cu ground state. The resulting picture for the relative placement of the three ^{70}Cu isomers is shown in Fig. 4.

Recent high-precision mass measurements on the ^{70}Cu isomers were performed with the Penning trap mass spectrometer ISOLTRAP [40,41] and have confirmed the placement of the three isomers in isomers ^{70}Cu. This leads us to the final conclusion that the ^{70}Cu ground state has a (6^-) spin and parity, the first isomeric state is situated at 101.1 keV with $I_\pi^+=(3^-)$, and the second isomeric state is at 242.4 keV with $I_\pi^+=1^+$.

F. Half-lives and production rates of the ^{70}Cu isomers

The half-life values for the 1^+ and (6^-) ^{70}Cu isomers were evaluated in this work using a high-statistics time spectrum, shown in part (a) of Fig. 5. It was taken with the 4π cylindrical plastic detector that is sensitive to β particles and to electrons from internal conversion. The decay period is sufficiently long ($\sim$2000 s) in order to correct for the ^{70}Ga background activity ($T_{1/2}$=21.15 min), present in the spectrum. Because of its low production rate (see below), the detected events from the decay of the (3^-) ^{70}Cu isomer could be neglected. The 1^+ and (6^-) ^{70}Cu half-lives are extracted from a fit containing a three-component exponential decay function and a constant background. The extracted half-life

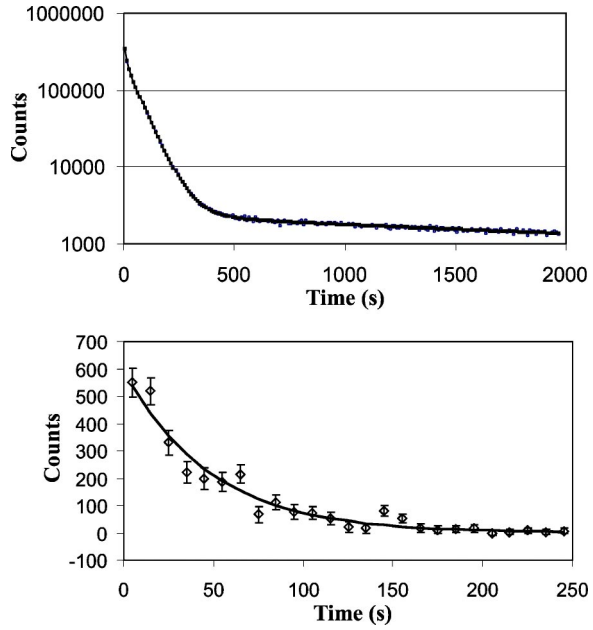

FIG. 5. Time dependence of the total counting rate in the 4π cylindrical β detector (a) and of the intensities of the 209, 387, 553, and 708 keV γ rays from the coincidence γ-ray spectra (b). The latter transitions come from the 3247 keV level and represent the decay of the ^{70}Cu (3^-) isomer. The solid lines are the result of a fit (see text).

values are 6.6(2) s and 44.5(2) s for the 1^+ and (6^-) ^{70}Cu isomers, respectively, and are summarized in Table III. Both values are consistent with the literature values. The half-life for the (3^-) ^{70}Cu isomer is derived from the time dependence of the intensities of the γ rays from the 3247 keV level in ^{70}Zn. The time spectrum is shown in part (b) of Fig. 5. The 3247 keV level is only populated by the (3^-) ^{70}Cu β decay, as shown in part (b) of Fig. 7. The fit with a single exponential decay function yields a half-life value of 33(2) s.

Using the above ^{70}Cu half-life values, the production rates of the three isomers could be derived. For this purpose, several γ-ray intensities were used. The resulting rates at the experimental setup are shown in Table III. These rates were determined during the neutron-induced fission experiment by implementing the Ta proton-to-neutron converter rod in the ISOLDE target. The rod was unable to withstand the high temperatures originating from the proton bombardment and was found twisted after the experiment [37]. This together with the use of the lasers in small bandwidth mode, resulting in a reduced laser power, explains the very low production rates compared to a rate of 9×10^7 μC^{-1} for ^{70}Cu (6^-), produced via proton-induced fission [30].

G. Decay scheme of ^{70}Ni

Knowing the relative placement of the three ^{70}Cu isomers, see Fig. 4, combined with the coincidence relations of the ^{70}Ni γ rays, see Table I, one is able to construct the ^{70}Ni decay scheme. The result is shown in Fig. 6.

When constructing the decay scheme, it is not clear at first which isomeric state(s) in ^{70}Cu is (are) populated by the β and β-delayed γ decay. Several levels however can be established and are clearly all decaying to the same final state. Most of these levels can decay to the final state by the emission of a single γ ray and hence it gives us a hint on the possible spin and parity of the final state. Since the ^{70}Ni ground state has $I^\pi=0^+$, only low spin states will be populated and thus the final state has to be the (1^+) isomeric state. A β feeding to the (1^+) isomeric state is further supported by the clear presence of the 141 keV isomeric transition in the singles spectrum from the ^{70}Ni decay (Fig. 1) and of other specific γ rays from the ^{70}Cu 1^+ β decay [e.g., the 186 and 874 keV γ rays, see part (a) of Fig. 7]. Notice that the 101 keV isomeric transition is not observed in the singles γ-ray spectra even though the 141 keV transition feeds directly the ^{70}Cu (3^-) isomeric state. However, this can be understood because the 101 keV transition is probably an $M3$ transition and thus highly converted ($\alpha=5.61$ [42]) and its apparent intensity is suppressed by the longer half-life compared to the 141 keV γ ray.

The γ-decay branch that goes via the 1611.2 keV transition happens with the emission of at least two γ rays and is therefore an exception to the above mentioned cases. It indicates a larger spin difference between the state fed in the β decay and the final states. Furthermore, the energies of the γ rays in coincidence with the 1611.2 keV γ ray—the 127.4, 140.4, and 267.8 keV transitions—correspond to the energy differences observed between the second and third, third and fourth, and second and fourth resonances in the $(t,{}^3\mathrm{He})$ reaction reported by Sherman *et al.* at energies of 100(6), 226(6) and 366(6) keV, respectively [19]. Since the state at 100(6) keV was already identified as being the (3^-) isomeric state in ^{70}Cu, it prompts us to place this γ-ray cascade feeding the (3^-) isomer in ^{70}Cu. It fixes new states at 228.5 and 368.9 keV which can be assigned as the 226(6) and 366(6) keV states by Sherman *et al.* Hence, the β decay of

TABLE III. Production rates ($\mathcal{P}$) at the experimental setup, experimental half-lives [$T_{1/2}$(expt.)], and half-lives from literature [$T_{1/2}$(lit.)] with its reference for the three ^{70}Cu isomers using the proton-to-neutron convertor method [37]. Note the lower production for the ^{70}Cu isomers because of technical problems with the convertor system and the use of reduced laser power during these measurements (see text).

Isomer	$\mathcal{P}(10^3$ at/μC)	$T_{1/2}$(expt.)(s)	$T_{1/2}$(lit.)(s)	Ref.
^{70}Cu 1^+	8(6)	6.6(2)	4.5(10)	[21]
^{70}Cu (3^-)	1.7(9)	33(2)		
^{70}Cu (6^-)	40(26)	44.5(2)	47(5)	[20]

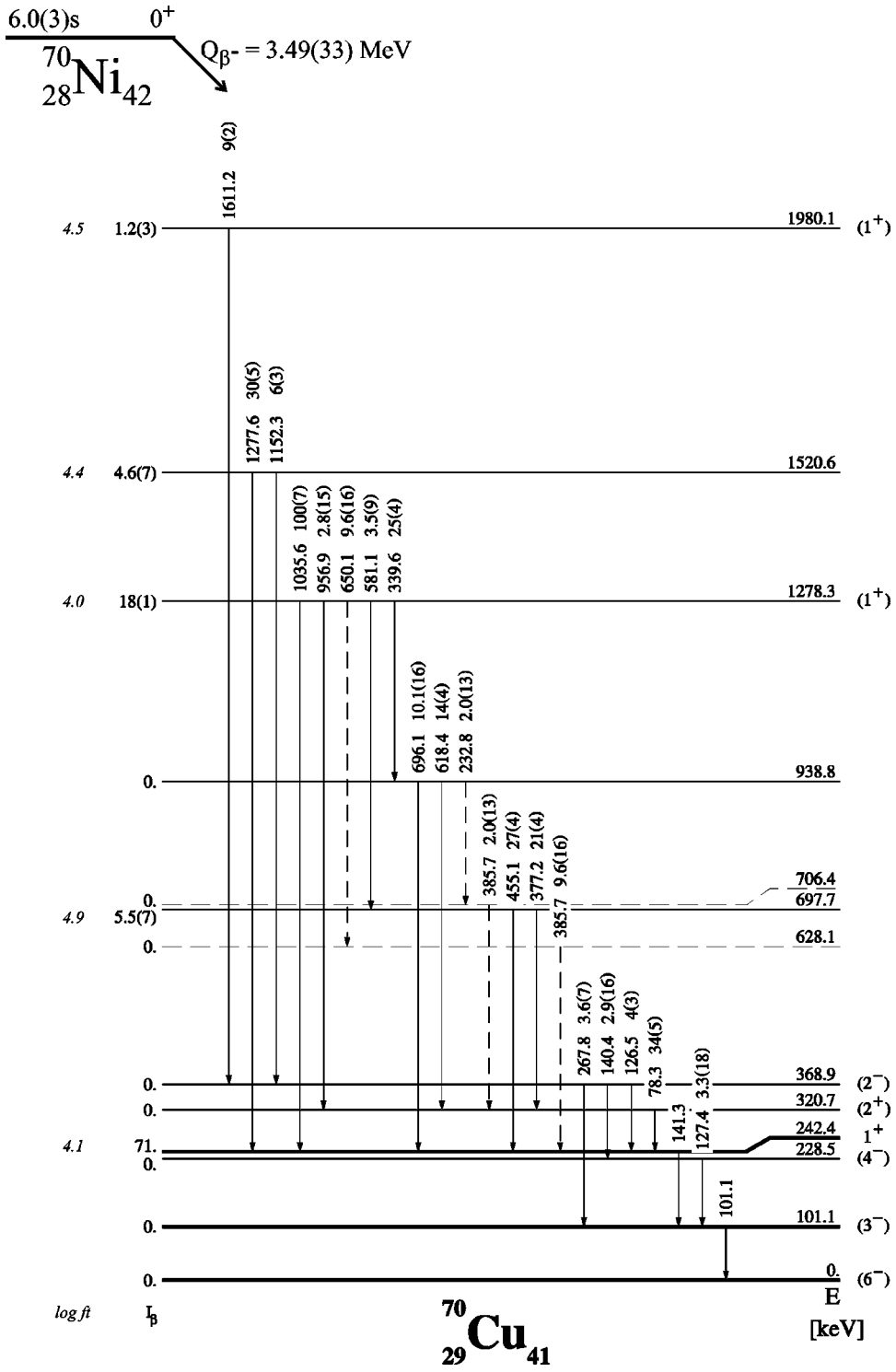

FIG. 6. Deduced decay scheme of ^{70}Ni. The half-life and Q_β values are taken from literature [12,38]. The 101.1 and 141.3 keV transitions are isomeric transitions. The order of the dashed γ-ray cascades is uncertain and might equally be reversed.

^{70}Ni breaks up in two parts: one dominant part that decays towards the ^{70}Cu isomer with $I^\pi = 1^+$ (98.8% of the β decay) and a weak branch that decays predominantly towards the ^{70}Cu (3^-) isomer via β feeding to a level at 1980.1 keV (1.2% of the β decay).

The γ rays at energies near 127, 140, and 386 keV were found to be doublets. The case for the doublet at $\sim$140 keV was already discussed above because of the observed isomeric transition at 141.3(3) keV between the (1^+) and (3^-) isomers in ^{70}Cu. The presence of a doublet near 127 and 386 keV is based on their coincidence relations with other γ rays, shown in Table I, and based on energy differences between the different existing levels. To discriminate between the two γ rays at 385.7(5) keV, we use the label "*t*" (top) and "*b*" (bottom) for the transitions leaving from the 706.4 and 628.1 keV levels, respectively. The order of the cascades of the 650.1−385.7(*t*) keV and 232.8−385.7(*b*) keV γ rays cannot be determined and might as well be reversed. Therefore, the γ rays and intermediate levels are shown as dashed lines.

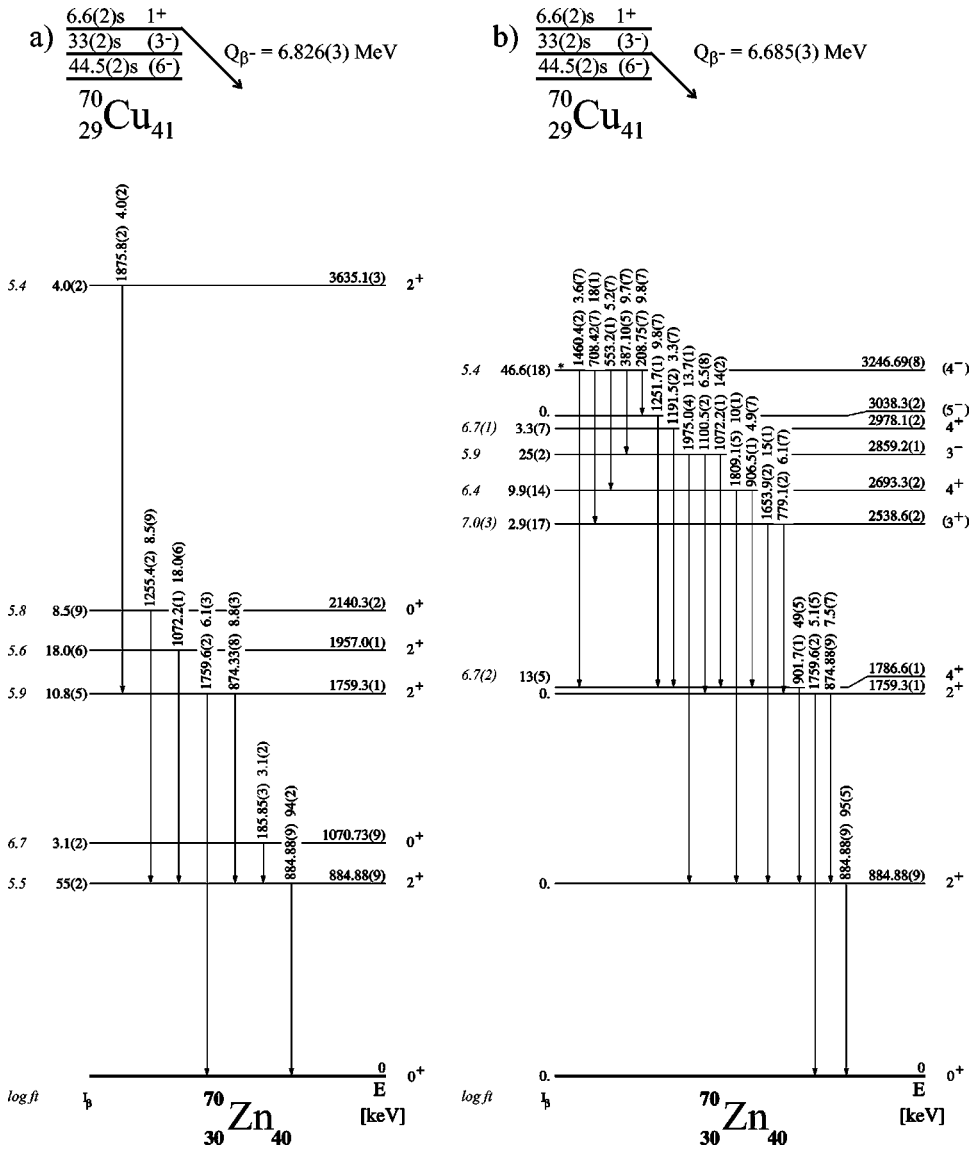

FIG. 7. Decay schemes of the three different ^{70}Cu isomers. (b) shows the decay of the newly identified isomer. The Q_β value is calculated using the mass excess values from literature [44] and from the recent ^{70}Cu mass measurement [40]. Levels not known in literature are labeled with "*."

The intensity balance of the γ rays was derived from the peak areas from the β-gated γ-ray spectra, correcting for the detection efficiency using the GEANT-simulated photopeak efficiency [43]. For some low-energy transitions, the multipolarity is known and these transitions are corrected for internal conversion, using Ref. [42]. The intensities of the transitions, with and without the internal conversion correction, are summarized in Table IV. The β-branching ratios and log *ft* values, shown in Fig. 6, are calculated from the intensities corrected for internal conversion. The β-branching ratio to the (1^+) isomeric state could not be derived from the γ-ray intensities but was derived by comparing the observed total ^{70}Ni β decay with the ^{70}Cu 1^+ daughter activity. The latter was derived by assuming an absolute intensity for the 885 keV transition in the ^{70}Cu 1^+ β decay to be 94(2)%. As will be shown further, this value corresponds with the assumption that the ^{70}Cu 1^+ isomer does not β decay to the ^{70}Zn ground state.

Spin and parity assignments of a number of levels were made. The level at 320.7 keV lies 78 keV above the 1^+ isomeric state and forms a good candidate for the 2^+ member of the $(1,2)^+$ doublet of the $\pi 2p_{3/2}\nu 2p_{1/2}^{-1}$ configuration. This case is similar to the ^{68}Cu neighbor, where a (2^+) state was found 84.6 keV above the 1^+ ground state [23]. Hence, we assign a tentative spin and parity of (2^+) to the 320.7 keV level. The level at 1278.3 keV is assigned an I^π of (1^+) because of its low log *ft* values (4.0) and because it feeds both the 1^+ and (2^+) states in ^{70}Cu. The level at 1980.1 keV is also assigned an I^π of (1^+), partly because of the low log *ft* value and partly because it decays further down in a two or three step process to the (3^-) isomeric state. In combination with the decay pattern of the intermediate 368.9 keV level, we propose tentative I^π values of (4^-) and (2^-) for the 228.5 and 368.9 keV levels, respectively. Note that the state at 228.5 keV was associated with the state at 226(6) keV from

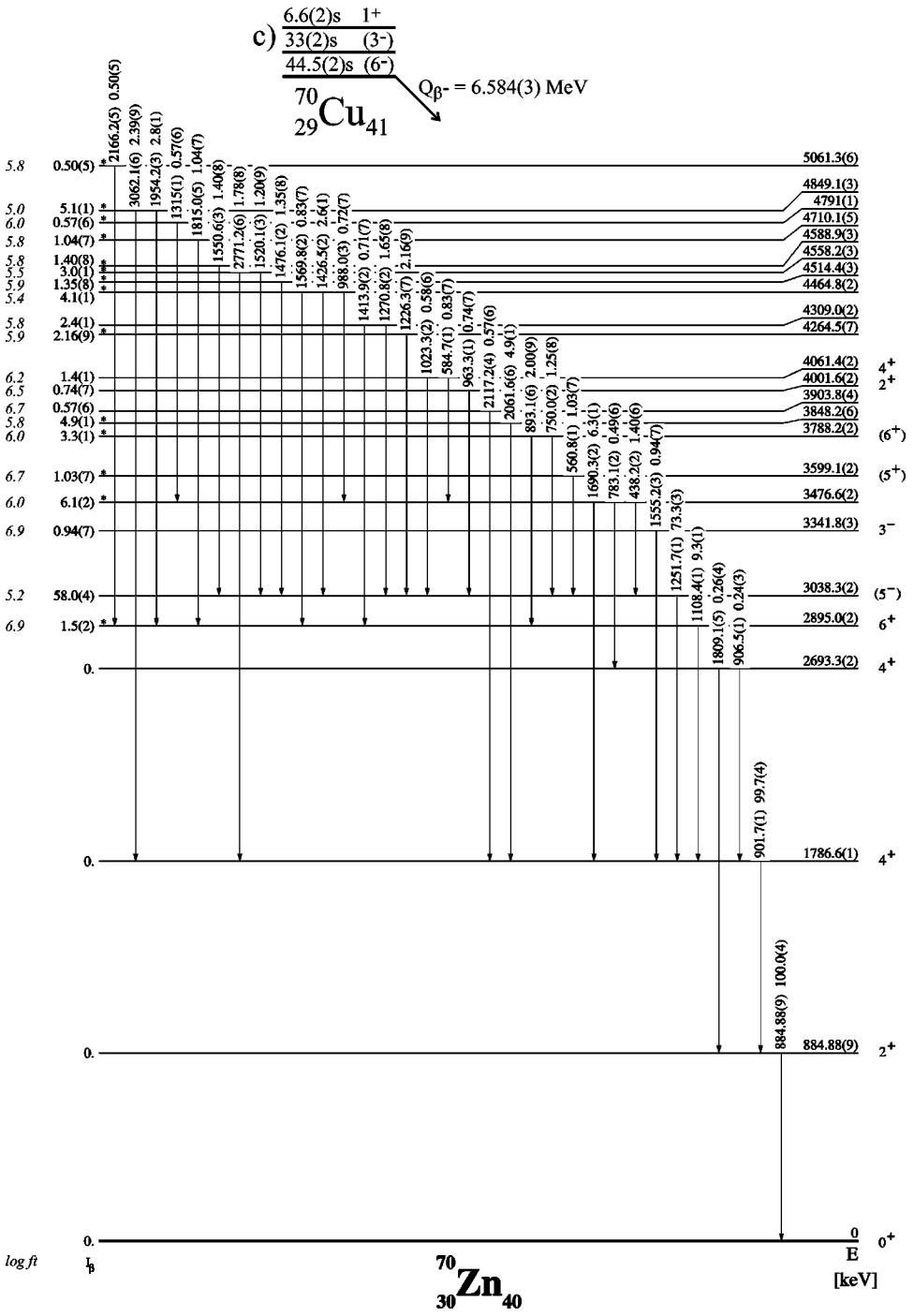

FIG. 7. (*Continued*).

the $(t,{}^3\mathrm{He})$ reaction reported by Sherman *et al.* [19] and it has been identified by the authors to be a member of the $(3-6)^-$ multiplet with the $\pi 2p_{3/2}\nu 1g_{9/2}$ configuration. It thus gives further support for the $(4)^-$ assignment.

H. Decay schemes of the ^{70}Cu isomers

Based on half-life considerations and the observed HFS of all the individual lines listed in Table II, the β decay of the three isomers in ^{70}Cu could be separated. Combined with the coincident γ-ray information from Table II, the different decay schemes were constructed. All 49 γ rays could be placed in one or several of the decay schemes and the complete decay schemes for the three ^{70}Cu isomers are shown in the corresponding parts of Fig. 7.

The intensity balance of the γ rays was derived from the peak areas from the singles spectra, correcting for the detection efficiency using the GEANT-simulated photopeak efficiency [43] and correcting the bypassing transitions for true summing effects. Based on the coincidence relations, the

1072 keV transition was found to be a doublet. The 1460 keV γ ray is a doublet with the ^{40}K background line and is corrected for by comparing it with the intensities from the β-gated spectra. The intensity values for the 101 and 141 keV isomeric transitions are also corrected for internal conversion [42] since these are low-energy transitions of higher multipolarity ($M3$ and $M2$, respectively). Some energy levels and γ-ray transitions are being populated in two or in all three ^{70}Cu decay schemes, and it is therefore impossible to unambiguously determine the β feeding from the different isomers to these levels. However, due to the differences in I^{π}, two different ^{70}Cu isomers cannot both decay via allowed β decay to the same energy level. The β feeding is therefore approximated by neglecting the first- and higher-forbidden contributions. The intensities of the transitions in the decay of the three isomers are summarized in Table V (normalized to the strongest transition) and in Fig. 7 (normalized to the total β decay). From the 101 and 141 keV intensities, the isomeric decay branching ratios could be extracted and are shown in Fig. 4. The branching ratio of the 141 keV isomeric transition could also be deduced from the ^{70}Ni decay and a good agreement with the value derived from the ^{70}Cu decay was found.

The β-decay branching ratios and log ft values were calculated using the intensity values from Table V. The β branching to the ^{70}Zn ground state cannot be determined via the γ-ray intensities. Only the ^{70a}Cu isomer is expected to decay to the 0^+ ^{70}Zn ground state because of its low spin assignment. The ground-state β feeding of the ^{70a}Cu isomer was deduced by Reiter *et al.* [21] to be 46(10)%. However, Franchoo *et al.* suggest a rather weak ground-state β feeding [8,12] based on the $^{68-74}$Ni cross-section measurements. The determination of the ^{70}Ni cross section has been derived by Franchoo *et al.* assuming no β feeding from the ^{70}Cu 1^+ isomer to the ^{70}Zn ground state. If instead the value of 46(10)% from literature would have been adopted, the production rate for ^{70}Ni would have been doubled. It was awkward to reconcile this result with the measured smooth cross-section behavior of the $^{68-74}$Ni isotopes. In our work, the ground-state β branching could not be determined since the ^{70}Cu 1^+ isomer is only weakly produced compared to ^{70}Cu (6^-). Instead, we will adopt the weak ground-state β feeding proposed by Franchoo *et al.* [8] and assume it to be zero. The quoted β-branching ratios and log ft values from part (a) of Fig. 7 should therefore be considered as upper (respectively lower) limits. The above assumption was also used in the derivation of the ^{70}Ni ground-state β branching (see above). A small direct feeding of the 1^+ isomer in ^{70}Cu to the 0^+ ground state in ^{70}Zn can be understood when considering the involved configurations (see Sec. III).

The I^{π} values shown in Fig. 7 are taken primarily from literature [6,38], except for the 2539, 3038, and 3247 keV levels. The 3247 and 3038 keV levels receive a large fraction of the β-decay strength (log ft=5.4 and 5.2, respectively) in the ^{70}Cu (3^-) and (6^-) β decay, respectively. It implies allowed decay, and hence it fixes the parity of both states to be negative and restricts the possible spin values (ΔI=0,1). There exists some disagreement about the spin of the 3038 keV level in literature. Although this level has been assigned as 4^- in the nuclear data sheets and I=4 in the table of isotopes [38,23], the results of (t,p) and (p,p) reaction studies [25,45] suggest a 5^- assignment for this level.[1] In contrast, in recent in-beam multinucleon transfer studies [6], a spin and parity of 4^+ was suggested, based on the observation of the 2154 keV transition from the 3038 keV level to the first excited 2^+ level. A γ line at this energy was also observed in our data but it was found to be a pure sum peak of the intense 1252 and 902 keV γ rays. Altogether, a spin of 5 for the 3038 keV level is a more reasonable assumption. Additional support for a spin of 5 comes from the fact that the (6^-) ^{70}Cu isomer can decay via allowed β decay to a 5^- state but it cannot do so to a 4^- state. We therefore assign a tentative spin and parity of (5^-) to this level. The spin and parity of the 3247 keV level are not known in literature. The allowed decay of the ^{70}Cu (3^-) isomer however restricts the spin to 2, 3, or 4. Spin 2 is excluded since the 209 keV γ ray would then be a delayed $M3$ transition to the (5^-) state at 3038 keV and this would cause the 209 keV transition to have a longer half-life. Furthermore, the level should also decay via fast $E1$ transitions to the two lowest 2^+ states but these transitions are not observed. A spin of 3 is also in conflict for similar reasons. A spin of 4 is consistent with the

TABLE IV. Relative γ-ray intensities (I_γ) and intensities corrected for internal conversion ($I_{\gamma+CE}$) for transitions in the decay of ^{70}Ni, normalized to the most intense transition. The lowest order multipolarity of the transition, used for the correction, is shown as well in case it is known. When the multipolarity is unknown, no conversion correction was applied.

E (keV)	I_γ	Multipolarity	$I_{\gamma+CE}$
78.3(1)	34(5)	$M1$	37(5)
126.5(2)	4(3)	$E1$	4(3)
127.4(2)	3.3(18)	$M1$	3.4(18)
140.4(6)	2.9(16)	$E2$	3.4(18)
232.8(3)	2.0(13)		2.0(13)
267.8(4)	3.6(7)	$M1$	3.6(7)
339.6(1)	25(4)		25(4)
377.2(1)	21(4)		21(4)
385.7(5)*t*	2.0(13)		2.0(13)
385.7(5)*b*	9.6(16)		9.6(16)
455.1(1)	27(4)		27(4)
581.1(2)	3.5(9)		3.5(9)
618.4(2)	14(4)		14(4)
650.1(2)	9.6(16)		9.6(16)
696.1(1)	10.1(16)		10.1(16)
956.9(3)	2.8(15)	$M1$	2.8(15)
1035.6(2)	100(7)		100(7)
1152.3(4)	6(3)		6(3)
1277.6(2)	30(5)		30(5)
1611.2(3)	9(2)		9(2)

[1] In the earlier evaluation of the nuclear data sheets, an I^{π} of 5^- was assigned for the 3038 keV level [46].

TABLE V. Relative intensities (I_{rel}) for the transitions in the decay of the three ^{70}Cu isomers. For each isomer, the normalization is such that the most intense transition has $I_{rel}=100$.

E (keV)	I_{rel}	E (keV)	I_{rel}	E (keV)	I_{rel}
		1072.2(1)	15(2)	1023.3(2)	0.58(6)
^{70}Cu 1^+ *decay*		1100.5(2)	6.8(8)	1108.41(1)	9.3(1)
141.3(3)	7.8(4)	1191.5(2)	3.5(7)	1226.3(7)	2.16(9)
185.85(3)	3.3(2)	1251.7(1)	10.4(7)	1251.7(1)	73.3(3)
874.33(8)	9.4(4)	1460.4(2)	3.8(8)	1270.8(2)	1.65(8)
884.88(9)	100(2)	1653.9(2)	16(1)	1315(1)	0.57(6)
1072.2(1)	19.2(6)	1759.6(2)	5.4(5)	1413.9(2)	0.71(7)
1255.4(2)	9(1)	1809.1(5)	11(1)	1426.5(2)	2.6(1)
1759.6(2)	6.5(3)	1975.0(4)	14(1)	1476.1(2)	1.35(8)
1875.8(2)	4.3(2)			1520.1(3)	1.20(9)
		^{70}Cu(6^-) *decay*		1550.6(3)	1.40(8)
^{70}Cu (3^-) *decay*		438.2(2)	1.40(6)	1555.2(3)	0.94(7)
101.1(3)	98(16)	560.82(8)	1.03(7)	1569.8(2)	0.83(7)
208.75(7)	10.4(7)	584.7(1)	0.83(7)	1690.3(2)	6.3(1)
387.10(5)	10.2(7)	750.0(2)	1.25(8)	1809.1(5)	0.26(4)
553.2(1)	5.4(7)	783.1(2)	0.49(6)	1815.0(5)	1.04(7)
708.42(7)	19(1)	884.88(9)	100.0(4)	1954.2(3)	2.8(1)
779.1(2)	6.4(7)	893.1(6)	2.00(9)	2061.6(6)	4.9(1)
874.33(8)	7.9(7)	901.7(1)	99.7(4)	2117.2(4)	0.57(6)
884.88(9)	100(5)	906.5(1)	0.24(3)	2166.2(5)	0.50(5)
901.7(1)	51(5)	963.3(1)	0.74(7)	2771.2(6)	1.78(8)
906.5(1)	5.2(8)	988.0(3)	0.72(7)	3062.1(6)	2.39(9)

observed γ rays, except for the decay to the 2538 keV level, which has $I^\pi=2^+$ according to the nuclear data sheets [38]. The spin of 2 is based on the $(n,n'\gamma)$ work from Refs. [24,47], although a 3^+ could not be excluded by the experimental error. Therefore, we assume the 2538 keV level to be a (3^+) state and the 3247 keV level a (4^-) state. An I^π of (4^-) of the 3247 keV level is also strongly supported by the shell-model description (see Sec. III).

III. DISCUSSION

A. Shell-model interpretation of excited states in ^{70}Cu

In the extreme shell-model picture, $^{70}_{29}Cu_{41}$ can be viewed as having one valence proton outside the $Z=28$ closed shell and one valence neutron outside the closed $N=40$ subshell. The experimental quasiparticle energies in the vicinity of the $^{68}_{28}Ni_{40}$ semidouble magic nucleus can be determined from the energy levels of the $^{69}_{29}Cu_{40}=^{68}_{28}Ni_{40}\otimes\pi$ and $^{69}_{28}Ni_{41}=^{68}_{28}Ni_{40}\otimes\nu$ nuclei, as shown in the left part of Fig. 8. The order of the excited states in ^{69}Cu is in agreement with the shell-model predictions for the $2p_{3/2}$, $1f_{5/2}$, $2p_{1/2}$, and $1g_{9/2}$ proton orbitals. The $\pi 1g_{9/2}$ orbital lies high up in energy, at 2553 keV, indicating the existence of the $Z=40$ subshell. The ^{69}Ni case is similar and the excited states correspond to holes in the νpf shell.

In ^{70}Cu, the valence proton and neutron will couple giving rise to a multiplet of states with spin values ranging from $(j_1^\pi+j_2^\nu)$ down to $|j_1^\pi-j_2^\nu|$ with j_i being the total angular momentum of orbital i. Due to the residual interaction, these states will split up in energy [48,18]. The energy will have a quadratic dependence on $I(I+1)$, with I being the spin, and thus $E_I=aI^2(I+1)^2+bI(I+1)+c$, i.e., the energy values lie on a parabola as a function of $I(I+1)$. Since it concerns both particles in ^{70}Cu, the parabola will be faced down, having one maximum for an intermediate spin value. The most important π-υ-coupling schemes are schematically drawn in Fig. 8.

A careful comparison with the levels observed in the β decay of ^{70}Ni (see Fig. 6) shows that the six lowest levels can be readily explained using this simple approach (see also Fig. 2 of Ref. [40]). The ^{70}Cu ground state and its first excited isomeric state at 101.1 keV were already attributed to the 6^- and 3^- members of the $\pi 2p_{3/2}\nu 1g_{9/2}$ multiplet. The other members are most probably the states at 226(6) and 506(6) keV according to Sherman *et al.* [19]. The 226(6) keV state was already associated with the (4^-) state at 228.5 keV observed in the ^{70}Ni decay. Hence the 506(6) keV state is most probably the (5^-) state. The $\pi 2p_{3/2}\nu 1g_{9/2}$ configuration is indeed expected to determine the lowest-energy states in ^{70}Cu since it is made by coupling the two orbitals that are lowest in energy. The (1^+) isomeric state at 242.4 keV and the (2^+) state at 320.7 keV were already proposed to be members of the $(1,2)^+$ doublet having the $\pi 2p_{3/2}\nu 2p_{1/2}^{-1}$ configuration. This configuration is indeed the

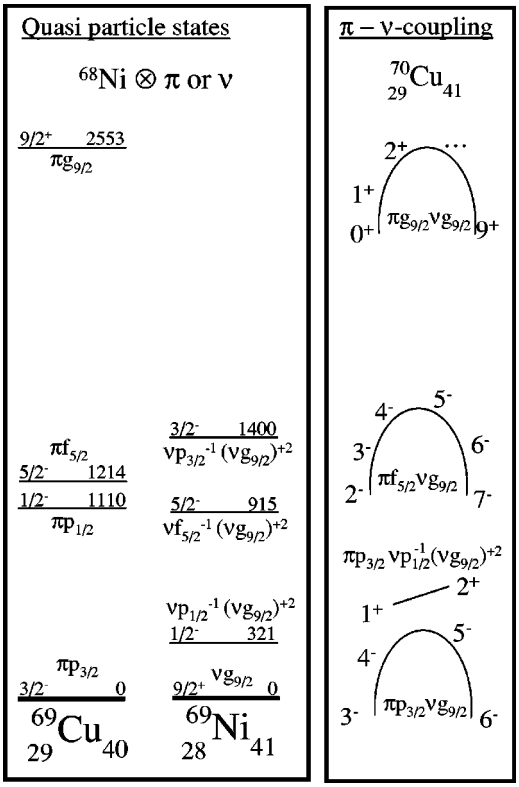

FIG. 8. Quasiparticle states in the vicinity of $^{68}_{28}Ni_{40}$ (left) and proton-neutron coupling schemes in $^{70}_{29}Cu_{41}$ (right).

second lowest in energy and is thus expected at energies of a few hundred keV.

To check the degree of purity of the lowest multiplets, we have performed shell-model calculations using ^{68}Ni as a core and a well-known zero-range interaction of the type [49,50]

$$V = -V_0\delta(\vec{r}_\pi - \vec{r}_\nu)(1 - \alpha + \alpha g\vec{\sigma}_\pi\vec{\sigma}_\nu), \qquad (1)$$

acting between the valence proton and valence neutron with the strength V_0=400 MeV fm^3 and α=0.1. These values of the parameters result in two-body matrix elements that come closest to those of the realistic interaction which will be described below, and they give a reasonable description of the spectrum of ^{58}Cu. The eigenvalues are shown in Fig. 9 and are compared with the part of the experimental data. Only the low-energy negative parity states can be discussed, since the excitation of neutrons from $\nu 2p_{1/2}$ orbital is not allowed in the chosen model space. In a good agreement with the discussion above, the lowest $(3^- - 6^-)$ states have dominant contribution of the $\pi 2p_{3/2}\nu 1g_{9/2}$ configuration (from 90% to 99%), while the second multiplet $(2^- - 7^-)$ arises mainly from the coupling of $\pi 1f_{5/2}$ and $\nu 1g_{9/2}$ orbitals ($\approx$80% for $4^-, 5^-$ states). The 6_2^- state lies at 1.1 MeV and is not seen at the scale of the figure. The inversion of the 3^- and 6^- states is not essential, since it is within the precision of the schematic shell model. The only possible 1^+ state in this model space corresponding to $\pi 1g_{9/2}\nu 1g_{9/2}$ configuration is positioned at 2.354 MeV, in rather good agreement with the experimental value of 1.980 MeV.

To validate further the predictions made and to get an insight into the structure of other possible states, we have also performed large-scale shell-model calculations using a realistic effective interaction as given by *G*-matrix calculation [51] with the modified monopole part [52]. The model space consists of the $(1f_{5/2}2p_{3/2}2p_{1/2}1g_{9/2})$ orbitals outside the ^{56}Ni core without any restrictions on their occupation.

The results of the diagonalization, performed with the shell-model code ANTOINE [53], are also shown in Fig. 9 and are in rather good agreement with the experimental data. The calculations show more mixing between the different configurations, however the main components of the lowest states can be clearly selected (see Table VI). As follows from this table, the contribution of the proposed $\pi 2p_{3/2}\nu 1g_{9/2}$ configuration in the first 6^-, 3^-, 4^-, and 5^- states is more than 52%, supporting the calculations using a more schematic force presented before. The second largest configuration is always $\pi 2p_{3/2}\nu(1f_{5/2}^{-2}1g_{9/2}^3)$ of about 18–20%. The contribution of other configurations does not exceed 6%.

The structure of the lowest 1^+ and 2^+ states is dominated by $\pi 2p_{3/2}\nu(2p_{1/2}^{-1}1g_{9/2}^2)$ configuration, with the second largest component being $\pi 2p_{3/2}\nu(1f_{5/2}^{-2}2p_{1/2}^{-1}1g_{9/2}^4)$ (see Table VI).

The calculated magnetic moments of the isomers are given in the last column of Table VI and are in very good agreement with the measured values [13].

The states, belonging in the extreme single-particle shell model, to the second negative parity multiplet, $(2^- - 7^-)$ from the $\pi 1f_{5/2}\nu 1g_{9/2}$ configuration, are predicted by the present realistic calculations to have more strongly mixed wave functions. The first 2^-,7^- states and the second $(3^- - 6^-)$ states placed by the calculation at energy between 1275 keV (for 2^- state) and 1797 keV (for 7^- state) do not contain a single-component contributing more than 18%. The same is valid for the next excited 1^+ states: all of them represent a complex mixture of many different pure configurations. Surprisingly, but in the present calculation (at least within the 10 lowest 1^+ states) we do not find the one with the dominant $\pi 1g_{9/2}\nu 1g_{9/2}$ configuration as seen experimentally for the 1^+ state at 1980.1 keV. The precise origin of this deficiency is not well understood as yet.

B. Shell-model interpretation of the ^{70}Ni β decay

As already mentioned, the ^{70}Ni β decay feeds directly the 1^+ ^{70a}Cu isomer and higher-lying states promptly γ decaying to two different isomers in ^{70}Cu, see Fig. 6. Most of the decay arrives at the ^{70a}Cu isomer but a weak decay branch also feeds the 1980.1 keV level (1.2% β branching) which further γ decays partly to the ^{70b}Cu isomer. Hence, the nickel decay can go through two different mechanisms that need to be interpreted.

The first mechanism for nickel to β decay is interpreted as a $\nu 2p_{1/2}$ neutron that is converted into a $\pi 2p_{3/2}$ proton. This is the most favorable allowed decay (Δl=0, with l being the orbital angular momentum) since the final configuration $\pi 2p_{3/2}\nu 2p_{1/2}^{-1}$ is low in energy (see Figs. 6 and 8). A substantial amount of all decays goes immediately to the (1^+) isomeric state (71%) and eventually all other decay will end up in this state as well because this is the lowest state having the

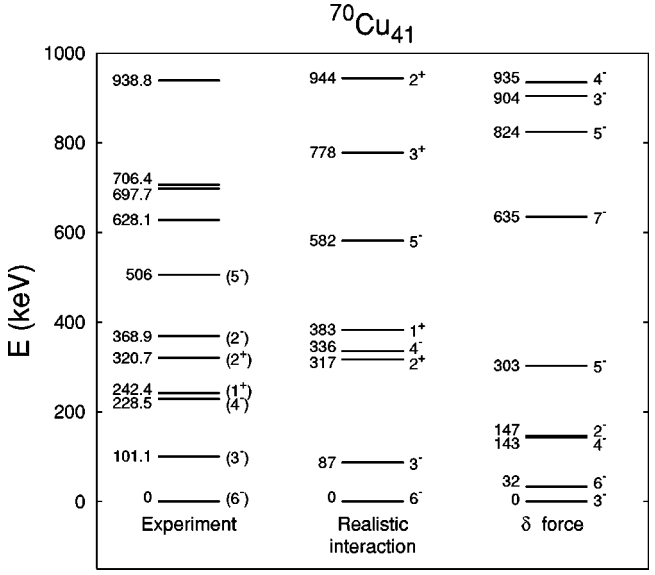

FIG. 9. Experimental and theoretical spectrum of $^{70}_{29}Cu_{41}$. See text for details.

$\pi 2p_{3/2}\nu 2p_{1/2}^{-1}$ configuration. The second mechanism for $^{70}_{28}Ni_{42}$ to decay is found by transforming a $\nu 1g_{9/2}$ neutron into a $\pi 1g_{9/2}$ proton. This is again of the allowed type but it is energetically less favorable since the copper daughter nucleus will only have a $\pi 1g_{9/2}\nu 1g_{9/2}$ configuration at high excitation energy. It gives rise to a $(0-9)^+$ multiplet, as shown in Figs. 6 and 8. However, due to the spin selection rules of allowed transitions, only the $(0,1)^+$ states can be populated by the 0^+ nickel ground state. The (1^+) level at 1980.1 keV is interpreted to be a member of this multiplet since it has high excitation energy and gets all the feeding in this decay branch. In order for this state to further deexcite, it is necessary that the proton moves to orbitals of lower energy. By lowering the proton from the $\pi 1g_{9/2}$ to the $\pi 1f_{5/2}$ orbital, the nuclei will arrive at the $\pi 1f_{5/2}\nu 1g_{9/2}$ configuration that is arranged in a $(2-7)^-$ multiplet. The 1611.2 keV γ ray can be interpreted as the transition to this configuration and the level at 368.9 keV as the (2^-) member of the $\pi 1f_{5/2}\nu 1g_{9/2}$ multiplet. The 368.5 keV level can further deexcite by lowering the proton from the $\pi 1f_{5/2}$ orbital to the $\pi 2p_{3/2}$ orbital. This leads to the population of the $(3,4,6)^-$ states having the $\pi 2p_{3/2}\nu 1g_{9/2}$ ground-state configuration. Note that states having the $\pi 2p_{1/2}\nu 1g_{9/2}$ configuration will not be populated in this decay although it would be energetically possible. However, these states will have $I^\pi=(4,5)^-$ and the spin selection rules thus prevent them from being populated. The γ ray at 126.5 keV forms an exception to the above story since it connects the (2^-) state with the (1^+) isomeric state. This transition cannot be interpreted in terms of simple single-particle transitions; the used shell-model picture is oversimplified and admixtures between different configurations should be included.

In this context, we have calculated the Gamow-Teller β-decay rates using the shell-model wave functions obtained from the large-scale shell-model calculations as described in the preceding section. In Table VII we present the theoretical B(GT) and log ft values, where

$$ft = \frac{K}{B(\mathrm{GT})}, \quad B(\mathrm{GT}) = \frac{1}{2I_i+1}(g_A/g_V)^2_{\mathrm{eff}}|\langle I_f||\hat{O}(\mathrm{GT})||I_i\rangle|^2, \tag{2}$$

calculated with $K=6260$ s, $(g_A/g_V)_{\mathrm{eff}}=0.74(g_A/g_V)$, $(g_A/g_V)=1.251$, and $\hat{O}$(GT) denoting the Gamow-Teller operator. The quenching factor of 0.74 is a standard choice for this mass region [54]. The agreement of the

TABLE VI. Structure of the lowest states in ^{70}Cu as follows from the shell-model calculations with the realistic effective interaction [51]. The magnetic moments of the isomers calculated with the effective spin g factors $[(g_s^{\pi,\nu})\mathrm{eff}=0.7(g_s^{\pi,\nu})\mathrm{free}]$ are given in the last column.

I^π	E_{expt} (keV)	E_{theor} (keV)	Configuration	(%)	μ_{expt} (μ_N) [13]	μ_{theor} (μ_N)
6^-	0	0	$\pi 2p_{3/2}\nu 1g_{9/2}$	(59)	(+)1.50(7)(8)	1.56
			$\pi 2p_{3/2}\nu(1f_{5/2}^{-2}1g_{9/2}^3)$	(18)		
3^-	101.1	87	$\pi 2p_{3/2}\nu 1g_{9/2}$	(56)	(−)3.50(7)(11)	−3.28
			$\pi 2p_{3/2}\nu(1f_{5/2}^{-2}1g_{9/2}^3)$	(18)		
4^-	228.5	336	$\pi 2p_{3/2}\nu 1g_{9/2}$	(52)		
			$\pi 2p_{3/2}\nu(1f_{5/2}^{-2}1g_{9/2}^3)$	(18)		
5^-	506.6	582	$\pi 2p_{3/2}\nu 1g_{9/2}$	(52)		
			$\pi 2p_{3/2}\nu(1f_{5/2}^{-2}1g_{9/2}^3)$	(20)		
2^-	368.9	1275	$\pi 1f_{5/2}\nu(2p_{1/2}^{-2}1g_{9/2}^3)$	(12)		
			$\pi 1f_{5/2}\nu(1f_{5/2}^{-2}1g_{9/2}^3)$	(12)		
			$\pi 2p_{3/2}\nu(1f_{5/2}^{-2}1g_{9/2}^3)$	(11)		
			$\pi 1f_{5/2}\nu 1g_{9/2}$	(10)		
1^+	242.4	383	$\pi 2p_{3/2}\nu(2p_{1/2}^{-1}1g_{9/2}^2)$	(51)	(+)1.86(4)(6)	2.20
			$\pi 2p_{3/2}\nu(1f_{5/2}^{-2}2p_{1/2}^{-1}1g_{9/2}^4)$	(14)		
2^+	320.7	317	$\pi 2p_{3/2}\nu(2p_{1/2}^{-1}1g_{9/2}^2)$	(49)		
			$\pi 2p_{3/2}\nu(1f_{5/2}^{-2}2p_{1/2}^{-1}1g_{9/2}^4)$	(13)		

TABLE VII. Theoretical and experimental log ft values of the Gamow-Teller β decay from ^{70}Ni to excited states in ^{70}Cu. The shell-model calculations have been performed with the realistic effective interaction [51,52].

I^{π}_{expt}	E_{expt}(keV)	I^{π}_{theor}	E_{theor} (keV)	$B(\text{GT})_{\text{expt}}$	$B(\text{GT})_{\text{theor}}$	$\log(ft)_{\text{expt}}$	$\log(ft)_{\text{theor}}$
1^+	242.4	1^+_1	383	0.497	0.439	4.1	4.15
	697.7	1^+_2	1044	0.079	0.067	4.9	4.97
(1^+)	1278.3	1^+_3	1594	0.626	0.767	4.0	3.91
	1520.6	1^+_4	1862	0.249	0.071	4.4	4.95
(1^+)	1980.1	1^+_5	2206	0.198	0.006	4.5	6.02

calculated and experimental values is remarkable for the three lowest states, and worsens for the transition rates to the 1521 and 1980 keV states for which the calculation seriously overestimates the B(GT) values extracted from the data.

C. Shell-model interpretation of the ^{70}Cu β decay

The β decay of the three isomers in ^{70}Cu, shown in Fig. 7, goes primarily to a few specific levels in ^{70}Zn. The ^{70}Cu 1^+ isomer decays mainly to the 2^+ states at 885 keV (log ft =5.5), 1957 keV (log ft=5.6), and 3635 keV (log ft=5.4), the ^{70}Cu (3^-) isomer to the (4^-) state at 3247 keV (log ft =5.4), and the ^{70}Cu (6^-) isomer decays primarily to the (5^-) state at 3038 keV (log ft=5.2) and to a few high-energy states at 4.5–5.0 MeV ($5.0 \leqslant \log ft \leqslant 5.5$). Most of these transitions and levels can be interpreted by the shell model.

The ^{70}Cu 1^+ isomer is mainly determined by a $\pi 2p_{3/2}\nu(2p^{-1}_{1/2}1g^{+2}_{9/2})$ configuration. The most favored allowed β decay will be the transformation of the $\nu p_{1/2}$ neutron into a $\pi 2p_{3/2}$ proton giving rise to the $\pi 2p^{+2}_{3/2}\nu 1g^{+2}_{9/2}$ configuration in ^{70}Zn, a pair excitation across the N=40 subshell. Hence, the 885 keV state will primarily have this configuration. As stated before, the experimental evidence out of the ^{70}Ni decay study points to only a small direct feeding to the ^{70}Zn ground state. This can be understood because the direct decay can only address the $\pi 2p^{-2}_{1/2}\nu 1g^{+2}_{9/2}$ component in ^{70}Zn which is apparently low. The state at 3635 keV cannot be interpreted to have the same configuration because this state does not decay to the 885 keV level, nor to the ^{70}Zn ground state. It implies that it is made up from a different configuration. Possibly, it is populated by the conversion of a $\nu 1g_{9/2}$ neutron into a $\pi 1g_{9/2}$ proton, resulting in a $\pi(2p_{3/2}1g_{9/2})\nu(2p^{-1}_{1/2}1g_{9/2})$ configuration. This configuration has four unpaired particles and is therefore expected at high energy. The observed decay of the 3635 keV state to the 1759 keV state cannot be interpreted as a single-particle transition because of spin and parity considerations.

The other ^{70}Cu isomers both belong to the $\pi 2p_{3/2}\nu 1g_{9/2}$ multiplet, shown in Fig. 8. The allowed β decay will transfer a $\nu p_{1/2}$ neutron into a $\pi 2p_{3/2}$ proton. This leads to a $\pi 2p^{+2}_{3/2}\nu(2p^{-1}_{1/2}1g_{9/2})$ configuration in zinc, giving rise to a $(4,5)^-$ doublet of states that can be associated with the 3247 and 3038 keV levels, respectively. In principle, both isomers should decay to both states. But due to the spin selection rules of allowed β decay (ΔI=0,1), the (6^-) copper isomer will only decay to the (5^-) zinc state and the (3^-) copper isomer is only allowed to decay to the (4^-) zinc state. It nicely explains the observed β-feeding pattern. The ^{70c}Cu β decay to the states around 4.5–5.0 MeV can be interpreted as the transformation of the uncoupled $\nu 1g_{9/2}$ neutron into a $\pi 1g_{9/2}$ proton, leading to the $\pi(2p_{3/2}1g_{9/2})\nu 2p^{+2}_{1/2}$ configuration.

D. The 101 and 141 keV isomeric transitions

The experimental partial half-lives for the 141 and 101 keV isomeric transitions are 97 s and 69 s, respectively. They can be compared with the theoretical Weisskopf estimates for $M2$ and $M3$ transitions, yielding 3×10^{-5} s (an $M2$ of 141 keV) and 300 s (an $M3$ of 101 keV) [23]. This gives for $B=T_{1/2}(\text{Weisskopf})/T_{1/2}(\text{exp})$ the values $B(141\text{ keV})=3\times10^{-7}$ and $B(101\text{ keV})=4.3$. Thus, for the 101 keV transition, the estimates predict the correct order of magnitude but for the 141 keV transition there is a difference of seven orders of magnitude between theory and experiment. The Weisskopf theory is however limited since it makes several assumptions [49] that do not hold for the ^{70}Cu nucleus. Nevertheless, the Weisskopf estimates are known to give good agreement with experiment over a wide range of the nuclear chart.

In order to explain the deviation of seven orders of magnitude, it is necessary to look at the shell-model description for multipole transitions in nuclei with two valence particles [50]. The reduced matrix element for an $M2$ operator between an initial 1^+ state in the $\pi 2p_{3/2}\nu 2p^{-1}_{1/2}$ configuration and a final 3^- state in the $\pi 2p_{3/2}\nu 1g_{9/2}$ configuration is found to be zero. Only an $M4$ operator leads to a nonvanishing transition probability. The Weisskopf estimate for the partial half-life of an $M4$ transition of 141 keV is in the order of 10^8 s, which is far too slow for the observed 97 s. It is clear that the states cannot be pure shell-model configurations but they are partially mixed, due to the residual interaction [50]. If the initial state is partially mixed with the $\pi 2p_{3/2}\nu 1f_{5/2}$ configuration, an $M2$ transition again becomes possible.

It is instructive to compare this case with the $^{68}_{29}\text{Cu}_{39}$ neighbor, having two neutrons less. In the shell-model picture, this nucleus has a valence proton in the $\pi 2p_{3/2}$ orbital and a valence neutron in the $\nu 2p_{1/2}$ orbital. The situation is very similar to ^{70}Cu: the low-lying positive parity states will mainly have the $\pi 2p_{3/2}\nu 2p_{1/2}$ configuration; the negative parity states will mainly have the $\pi 2p_{3/2}\nu 1g_{9/2}$ configuration. An $M2$ transition from the 3^- state at 610.5 keV to the 1^+-ground state is observed but it is not delayed [23]. The

Weisskopf estimates for an $M2$ transition of 610 keV are in the order of 10^{-8} s and thus agree roughly with the observations. However, since the shell-model configurations of the 3^- and 1^+ states are believed to be the same as in ^{70}Cu, the transition matrix element for an $M2$ should vanish and only an $M4$ transition is allowed by the theory. To explain the observed fast half-life, it is necessary to assume also here a strong $\nu 1f_{5/2}$ admixture in the ground-state wave function.

IV. CONCLUSION

The complementarity of the LISOL and ISOLDE facilities has nicely been demonstrated by presenting the results from a β-decay study of both ^{70}Ni and ^{70}Cu. In addition, the power of the in-source laser spectroscopy method in combination with conventional decay spectroscopy has been shown as well since it has yielded the identification and a clear separation of a new third β-decaying isomer in ^{70}Cu. The experimental results could be combined in a consistent way.

The shell-model description of the ^{70}Cu nucleus in the picture of a ^{68}Ni core plus two valence nucleons provide a good basis to explain the existence of the three isomers and to describe the different branches in the ^{70}Ni β decay to the ^{70}Cu 1^+ and (3^-) isomers and their subsequent β decay to specific excited states in the ^{70}Zn nucleus. It allowed the determination of the dominant shell-model configurations of the ground state and several excited states in ^{70}Cu and in ^{70}Zn. A large-scale shell-model calculation using realistic effective interactions was performed and allowed a more detailed insight into the main configurations of the low-lying states of ^{70}Ni. It showed that the $(6^-,3^-,4^-,5^-)$ states from the lowest multiplet contain about 50% of the $\pi 2p_{3/2}\nu 1g_{9/2}$ configuration, but also that at least 33% stems from a neutron $2p$-$2h$ configuration through the $N=40$ subshell closure. A similar conclusion was drawn for the $(1^+,2^+)$ multiplet. All other states appear to be strongly mixed and the calculation could not reproduce the 1980 keV (1^+) state that according to its feeding and decay characteristics should be of rather pure character. The latter forms a challenge for the effective interactions used in the region of the chart of nuclei. The results presented in this work indicate the existence of a rather weak subshell closure at $N=40$ and the ^{68}Ni core therefore cannot be treated fully as an inert core.

ACKNOWLEDGMENTS

We gratefully thank J. Gentens and P. Van den Bergh for running the LISOL separator. We would like to acknowledge the ISOLDE technical group for assistance during the experiment. N.A.S. thanks E. Caurier and F. Nowacki from IReS (Strasbourg) for making available their shell-model code and interaction, and for useful discussions. This work was supported by the Inter-University Attraction Poles (IUAP) under Project No. P5/07 and the FWO-Vlaanderen, Belgium.

[1] R. Broda *et al.*, Phys. Rev. Lett. **74**, 868 (1995).
[2] F. Ameil *et al.*, Eur. Phys. J. A **1**, 275 (1998).
[3] R. Grzywacz *et al.*, Phys. Rev. Lett. **81**, 766 (1998).
[4] J. I. Prisciandaro *et al.*, Phys. Rev. C **60**, 054307 (1999).
[5] T. Ishii *et al.*, Phys. Rev. Lett. **84**, 39 (1999).
[6] A. N. Wilson *et al.*, Eur. Phys. J. A **9**, 183 (2000).
[7] O. Sorlin *et al.*, Phys. Rev. Lett. **88**, 092501 (2002).
[8] S. Franchoo *et al.*, Phys. Rev. Lett. **81**, 3100 (1998).
[9] L. Weissman *et al.*, Phys. Rev. C **59**, 2004 (1999).
[10] W. F. Mueller *et al.*, Phys. Rev. Lett. **83**, 3613 (1999).
[11] W. F. Mueller *et al.*, Phys. Rev. C **61**, 054308 (2000).
[12] S. Franchoo *et al.*, Phys. Rev. C **64**, 054308 (2001).
[13] L. Weissman *et al.*, Phys. Rev. C **65**, 024315 (2002).
[14] A. M. Oros-Puesquens and P. F. Mantica, Nucl. Phys. **A669**, 8 (2000).
[15] K. Langanke *et al.*, Phys. Rev. C **67**, 044314 (2003).
[16] K. Langanke *et al.*, Phys. Rev. Lett. **90**, 241102 (2003).
[17] H. Grawe *et al.*, in Tours Symposium on Nuclear Physics IV, Tours 2000, edited by M. Arnould, M. Lewitowicz, Yu Ts. Oganessian, H. Akimune, M. Ohta, H. Utsunomiya, T. Wada, and T. Yamagata, AIP Conf. Proc. 561 (AIP, Melville, NY, 2001), p. 287.
[18] V. Paar *et al.*, Nucl. Phys. **A331**, 16 (1979).
[19] J. D. Sherman *et al.*, Phys. Lett. **67B**, 275 (1977).
[20] L. M. Taff *et al.*, Nucl. Phys. **A164**, 565 (1971).
[21] W. L. Reiter *et al.*, Nucl. Phys. **A249**, 166 (1975).
[22] E. Runte *et al.*, Nucl. Phys. **A399**, 163 (1983).
[23] R. Firestone, *Table of Isotopes*, 8th ed. (Wiley, New York, 1996).
[24] Yu. G. Kosyak *et al.*, Izv. Akad. Nauk SSSR, Ser. Fiz. **46**, 2257 (1982).
[25] F. R. Hudson *et al.*, Nucl. Phys. **A189**, 264 (1972).
[26] S. Leenhardt *et al.*, Eur. Phys. J. A **14**, 1 (2002).
[27] E. Kugler *et al.*, Hyperfine Interact. **129**, 23 (2000).
[28] V. I. Mishin *et al.*, Nucl. Instrum. Methods Phys. Res. B **73**, 550 (1993).
[29] V. F. Fedoseyev *et al.*, Hyperfine Interact. **127**, 409 (2000).
[30] U. Köster *et al.*, Ph.D. thesis, TU München, Germany, 2000.
[31] Y. Kudryavtsev *et al.*, Nucl. Instrum. Methods Phys. Res. B **114**, 350 (1996).
[32] K. Kruglov *et al.*, Eur. Phys. J. A **14**, 365 (2002).
[33] K. Kruglov *et al.*, Eur. Phys. J. A **14**, 365 (2002).
[34] U. Köster *et al.*, Nucl. Instrum. Methods Phys. Res. B **160**, 528 (2000).
[35] U. Köster *et al.*, Hyperfine Interact. **127**, 417 (2000).
[36] K. Kratz *et al.*, Z. Phys. A **340**, 419 (1991).
[37] R. Catherall *et al.*, Nucl. Instrum. Methods Phys. Res. B **204**, 235 (2003).
[38] M. R. Bhat, Nucl. Data Sheets **68**, 124 (1993).
[39] T. Ishii *et al.*, Phys. Rev. Lett. **81**, 4100 (1998).
[40] J. Van Roosbroeck *et al.*, Phys. Rev. Lett. (in press).
[41] F. Herfurth *et al.*, J. Phys. B **36**, 931 (2003).
[42] I. M. Band, M. B. Trzhaskovskaya, and M. A. Listengarten, At. Data Nucl. Data Tables **18**, 433 (1976).
[43] GEANT 3.21—Detector Description and Simulation Tool, CERN, Geneva (1993), http://wwwinfo.cern.ch/asd/geant/

[44] G. Audi and A. H. Wapstra, Nucl. Phys. **A595**, 1 (1995).
[45] J. Jabbour *et al.*, Nucl. Phys. **A464**, 287 (1987).
[46] F. Kearn and J. N. Mo, Nucl. Data Sheets **25**, 1 (1978).
[47] Yu. G. Kosyak *et al.*, Izv. Akad. Nauk SSSR, Ser. Fiz. **49**, 2118 (1985).
[48] M. H. Brennan and A. M. Bernstein, Phys. Rev. **120**, 927 (1960).
[49] P. J. Brussaard and P. W. M. Glaudemans, *Shell-model Applications in Nuclear Spectroscopy* (North-Holland, Amsterdam, 1977).
[50] K. L. G. Heyde, *The Nuclear Shell Model* (Springer-Verlag, Berlin, 1990).
[51] M. Hjorth-Jensen, T. T. S. Kuo, and E. Osnes, Phys. Rep. **261**, 125 (1995).
[52] F. Nowacki, Ph.D. thesis, IReS, Strasbourg, 1996; F. Nowacki (private communication).
[53] E. Caurier, shell model code ANTOINE, IReS, Strasbourg, 1989–2002; E. Caurier and F. Nowacki, Acta Phys. Pol. B **30**, 705 (1999).
[54] K. Langanke *et al.*, Phys. Rev. C **52**, 718 (1995).